Plastic Enclave Sizes for Internal Cracks Emanating from Circular Cavities within Elastic Plates*

Thomas Rich

June 1967

Progress Report Prepared for NASA under Contract NGR 39-007-011

Lehigh University

Bethlehem, Pa.

* This work was partially supported by NASA under contract NGR 39-007-011 and NSF Grants GK-344 and GK-1164.

TABLE OF CONTENTS

List of Figures

List of Tables

Abstract

This thesis presents an analytical method, which employs a numerical solution, for the estimation of the plastic enclave size at the tip of a crack emanating from an edge or an internal cavity within an elastic plate under various loading conditions. The representative plastic enclave length is based upon the Dugdale Plastic Zone Model. The complex stress function approach of Muskhelishvili in conjunction with conformal mapping techniques is employed to determine the enclave size.

To demonstrate this analytical method, the plastic enclave sizes are estimated for single and twin symmetrically located radial cracks emanating from a circular void within an elastic plate under uniform uniaxial tension. The resulting stress intensity data and plastic enclave sizes are presented in tabular and graphical form for a wide range of crack dimensions and tensile loads. From numerical convergence tests on the results, the data is judged to be accurate to within 2%.

Discussion is presented concerning the application of the analytical method to estimating plastic enclave sizes for a wide variety of problems. Finally, an experimental approach for the verification of analytical results is proposed which employs reflective photoelastic techniques.

I. Introduction

The presence of cracks and flaws directly influences the strength characteristics of elastic materials. One approach to the understanding of this phenomenon has been the study of the elastic stress field adjacent to the crack tip. Paris and Sih [1][1] report the stress fields as developed by Irwin for the three basic modes of crack surface displacement. Refer to Fig. 1. In mode I, the opening mode, the crack surfaces move directly apart. In mode II, the edge sliding mode, the crack surfaces slide over each other perpendicular to the leading edge. In mode III, the tearing mode, the crack surfaces slide with respect to one another parallel to the leading edge.

The Irwin stress expressions for mode I are

$$\sigma_x = \frac{K}{\sqrt{2r}} \cos\frac{\theta}{2}\left[1 - \sin\frac{\theta}{2}\sin\frac{3\theta}{2}\right]$$
$$\sigma_y = \frac{K}{\sqrt{2r}} \cos\frac{\theta}{2}\left[1 + \sin\frac{\theta}{2}\sin\frac{3\theta}{2}\right] \qquad (1)$$
$$\tau_{xy} = \frac{K}{\sqrt{2r}} \sin\frac{\theta}{2}\left[\cos\frac{\theta}{2}\cos\frac{3\theta}{2}\right]$$

plus higher order terms in r, where the corresponding

[1] Numbers in brackets designate references at the end of this thesis

coordinate notation is illustrated in Fig. 2. The parameter, K, in the equations is termed the stress intensity factor. It is independent of the r and θ coordinates but does depend upon the magnitude of the loading force and the geometric dimensions of the body including the crack length. The stress intensity factor is a physical measure of the amount of force transmitted throught the crack tip area.

Inspection of eqs. (1) reveals a singularity in the stresses as r approaches zero. This condition is physically impossible, and therefore, there must be some relaxation of these "infinite stresses" near the crack tip through the mechanism of plastic yielding. The zone, which is adjacent to the crack tip and in which this yielding occurs, is defined as the plastic enclave.

Irwin [2] suggests an initial approximation for the plastic enclave size. The normal stress, which acts along the line of expected crack extension, is given by eqs. (1), for $\theta = 0$:

$$\sigma_y = \frac{K}{\sqrt{2r}}$$

By solving for r when σ_y equals the yield stress, Y, of the participating material subjected to simple tension, one obtains

$$r_{ys} = \frac{1}{2}\left(\frac{K}{Y}\right)^2 \qquad (2)$$

Irwin admits that r_{ys} is only a rough estimation of the plastic enclave size but indicates its importance for proposing a criterion for the minimum toughness of a structure against fracture failure caused by small flaws.

Significant progress towards the estimation of plastic zone size has been made by Dugdale [3]. He suggests a physical model of the plastic enclave wherein a linear elasticity approach can be employed to the non-linear plasticity effect. Referring to Fig. 3, for a very thin sheet containing a crack and loaded perpendicular to the crack line, plastic yielding is assumed to occur in a strip of elastic-perfectly plastic material, which precedes the crack tip in a direction coincident with the crack line. Thus, according to Dugdale's model the plastic enclave is an extension of the initial crack by a length, W, which becomes larger with an increase in external load and upon which normal tensile stresses act equal in magnitude to the material yield stress, Y. Dugdale then represents the normal stress, σ_y, acting at the enclave edge, by the linear superposition of the stresses resulting from the plastic load, Y, and the external load, σ_∞. He states that the Y and σ_∞ contribution to σ_y can be determined in the form of series

in ascending powers of α having the leading terms:

$$\sigma_{y_\gamma} = -2\gamma\beta/\pi\alpha$$
$$\sigma_{y_\infty} = \sigma_\infty/\alpha \qquad (3)$$

where α and β are defined by

$$x = L\cosh\alpha \quad , \quad a = L\cos\beta$$

By setting the combination of the coefficients of α^{-1} equal to zero, Dugdale provides a condition by which the stress singularity at $\alpha = 0$, $x = L$, is removed, i.e.:

$$\sigma_\infty - 2\gamma\beta/\pi = 0 \qquad (4)$$

The condition (4) can be manipulated into an expression from which the plastic enclave size can be estimated for any given load to yield ratio and initial crack length. It is

$$\frac{W}{L} = 2\sin^2\left(\frac{\pi}{4}\frac{\sigma_\infty}{Y}\right) \qquad (5)$$

and the corresponding plastic enclave size is given by

$$w = a\frac{W}{L}\Big/\left(1-\frac{W}{L}\right) \qquad (6)$$

He has also conducted experiments with steel sheets subjected to uniaxial tension perpendicular to internal slits which tend to verify his analytical approximation.

Rosenfield, Dai, and Hahn [4] describe experiments which reveal the three-dimensional nature of the plastic enclaves preceding notches and cracks in steel plates under tension. Their findings help to substantiate the Dugdale model as a fair representation of actual physical plastic enclaves. From their experimental results, the plastic zone appears to be a wedge shaped plane inclined at 45 degrees to the plane of the crack as illustrated in Fig. 4. They suggest that the inclined plastic wedge under plane stress conditions can be interpreted in terms of the Dugdale horizontal plastic wedge, and the differences between them diminish as the plastic enclave size surpasses the plate thickness. They conclude that by transforming the three-dimensional plastic region into a one-dimensional plastic zone, the Dugdale model vastly reduces the analytical complexity of the problem, and therefore any inaccuracies introduced by its use are tolerable.

One of the cases where the Dugdale model and resulting plastic zone sizes are fruitfully employed is the plasticity correction to the stress intensity factors for a single-edge cracked specimen in tension as developed by Kobayashi and Brown [5]. The resulting stress intensity factors for various crack length to specimen width ratios are consistently larger than those obtained by elastic analysis and agree with experimental

findings.

This thesis has been undertaken to extend Dugdale's model to the estimation of plastic enclave sizes in the more complex problem of cracks emanating from voids within elastic plates. An analytical technique is developed by which the Dugdale model can be applied to a wide variety of geometries and load conditions. To achieve this end, the Muskhelishvili [6] complex variable approach to plane elasticity in conjunction with conformal mapping methods are applied to the problem. The stress intensity factors obtained from the elasticity solution are dependent upon the plastic enclave size as defined by Dugdale's model. For each set of geometric and loading conditions, the plastic enclave size is determined such that the resulting stress intensity factor vanishes and no "infinite stresses" exist in the crack tip region. A specific detailed problem is given where the plastic enclave sizes are estimated for internal cracks emanating from circular cavities within elastic plates under tension. The solution for the enclave sizes of related problems is discussed with respect to the method presented in this thesis, and an experimental verification technique is proposed employing photoelasticity.

II. Analytical Development

2.1 General Approach

The estimation of the plastic enclave sizes at the leading edges of internal cracks emanating from a circular cavity within an infinite elastic sheet is given to present an analytical method by which Dugdale's model can be extended to complex geometries. The elastic sheet is subjected to a uniform uniaxial tensile load applied at infinity. The two specific cases presented are shown in Fig. 5: a single and a twin crack geometry. The problem is immediately separated into the linear superposition of the case with only external loads, problem A, and that with only plastic loads, problem B, as illustrated in Fig. 6. In this manner the stress intensity factor at a plastic enclave tip, L, can be determined as the contribution from the external load plus that from the plastic load. The plastic enclave will then be the length, W, for which

$$K = K_A + K_B = 0 \qquad (7)$$

This insures that the stresses in the crack tip region remain finite. The stress intensity factors, K_A, have been reported by Roberts and Rich [7]. They employed the complex variable techniques of Muskhelishvili [6]

in a manner similar to the one explained next for the determination of K_B.

A conformal mapping function is used which transforms the circular void with k symmetrically emanating radial cracks and the infinite complex z plane exterior to the void and cracks onto a unit circle and exterior infinite ζ plane. The functional representation of this transformation is

$$z = \omega(\zeta) \tag{8}$$

where W is then expanded into an infinite polynomial series in ζ. This transformation provides a simpler geometry upon which the boundary conditions from the plastic enclave may be applied.

At this point, two complex stress functions, φ and ψ, which are holomorphic in the region exterior to the unit circle, are defined in the ζ plane. The elastic stresses in this region are given by Muskhelishvili as

$$\widehat{\rho\rho} + \widehat{\theta\theta} = 4\,\mathrm{Re}\,\varphi'(\zeta) \tag{9}$$

$$\widehat{\theta\theta} - \widehat{\rho\rho} + 2i\widehat{\rho\theta} = \left(\zeta^2/\overline{\omega'(\zeta)}\right)\left[\overline{\omega(\zeta)}\,\varphi''(\zeta) + \omega'(\zeta)\,\psi'(\zeta)\right]$$

where $\widehat{\rho\rho}$ and $\widehat{\theta\theta}$ are the normal stress components and $\widehat{\rho\theta}$ is the shear component in polar coordinates. From the stress function $\varphi(\zeta)$, the stress intensity factor at a crack tip, $\zeta = \eta$, is obtained using the expression

given by Paris and Sih [1]:

$$K_B = 2\sqrt{2} \lim_{\zeta \to \eta} \left[\omega(\zeta) - \omega(\eta)\right]^{1/2} \frac{\varphi'(\zeta)}{\omega'(\zeta)} \tag{10}$$

Because only $\varphi(\zeta)$ is involved in (10), it is the only stress function which needs to be determined.

For this boundary value problem of the first kind, the surface tractions are specified at the boundary and are related to the stress functions by the transformed boundary equation as given in [6]:

$$\varphi(\zeta) + \frac{\omega(\zeta)}{\overline{\omega'(\zeta)}} \overline{\varphi'(\zeta)} + \overline{\psi(\zeta)} = f_1 + i f_2 \tag{11}$$

where $f_1 + if_2$ represents the loading function in the plastic zone. Muskhelishvili [6] gives the contour integral for the loading function as

$$f_1 + i f_2 = i \int_L (x_n + i y_n)\, ds \tag{12}$$

where x_n and y_n are the vector components of the external tractions which act along the boundary, L.

When the surface traction is a constant normal stress, which is precisely the problem B where Y acts over the crack surface corresponding to the enclave length, the same reference shows

$$-i \int_L (x_n + i y_n)\, ds = Yz \tag{13}$$

where L corresponds to the circular edge plus adjoining crack-(s) in the z plane. Then the loading function is transformed to the ζ plane and expanded into a

complex Fourier series by

$$f_1 + i f_2 = \frac{1}{2\pi}\int_0^{2\pi} Y(\theta) e^{-i\eta\theta} d\theta = \sum_{-\infty}^{\infty} d_n \zeta^n \qquad (14)$$

where $Y(\theta)$ is the transformed function, which is expressed in polar form and integrated clockwise along the unit circle, θ is the polar angle in the ζ plane, and d_n is the resulting Fourier coefficient.

By substituting $f_1 + if_2$ as a Fourier Series, $\omega(\zeta)$ expressed as an infinite polynomial, $\varphi(\zeta)$ and $\psi(\zeta)$ written as Laurent Series about $\zeta = 0$, into (11), an infinite set of linear algebraic equations is obtained for the determination of the coefficients of $\varphi(\zeta)$. To obtain a practical solution for $\varphi(\zeta)$, the infinite set of equations is approximated by its **partitioned set**, which consists of the first M equations in the first M coefficients of $\varphi(\zeta)$. This is accomplished by truncating $\omega(\zeta)$ to a series of N terms before applying it to (11). The problem therefore reduces to the numerical solution of (11) for the coefficients of $\varphi(\zeta)$. Studies are also required to learn the effect of truncating $\omega(\zeta)$ on $\varphi(\zeta)$'s convergence. From the coefficients, $\varphi'(\zeta)$ is easily obtained and substituted back into (10) for K_B.

Using the values of K_A and K_B, which are determined for a wide range of σ_∞/γ and L/R ratios, in conjunction with condition (7), the Dugdale plastic zone sizes for various ranges of the same parameters are determined.

In the following detailed solution, all coefficients for the various series were computed by recursion loops on a digital computer. Refer to the program listing in Appendix C for the specific procedures used to calculate any particular set of coefficients.

2.2 Mapping Function

The mapping function which was used to map the circular void with k symmetrically emanating radial cracks and the infinite complex z plane, which is exterior to the void and cracks, onto a unit circle and exterior infinite complex ζ plane is given by Roberts and Rich [7] as

$$Z = \left\{ \frac{1}{1-\epsilon} \left[\zeta^{k} + \zeta^{-k} + 1 + \epsilon + (1+\zeta^{-k})(\zeta^{2k} + 2\epsilon\zeta^{k} + 1)^{1/2} \right] \right\}^{1/k} \qquad (15)$$

where k=1 corresponds to the single crack problem; k=2 corresponds to the twin crack problem. The parameter, ϵ , is a real number which depends upon the crack length to void radius ratio, L/R. The Z plane and corresponding ζ plane for both k=1 and 2 are shown in Fig. 7. In both cases $\omega(\zeta)$ maps the cracks as branch cuts.

Derivations of the following important properties of the mapping functions are given in Appendix A. The constant, $\frac{1}{1-\epsilon}$, was chosen in (15) to normalize the geometry with respect to R in the Z plane. Thus for a given value of L/R in the physical problem, the value of L in the Z plane is set equal to that ratio. The parameter, ϵ , is related to L by

for k=1

$$\epsilon = 2\left(\frac{L}{L+2}\right)^2 - 1 \qquad (16)$$

k=2

$$\epsilon = 2\left(\frac{\lambda^2-1}{\lambda^2+1}\right)^2 - 1$$

where $\lambda = L + 1$ and ϵ varies from + 1 when L approaches infinity to - 1 when L approaches zero.

Referring again to Fig. 7, the transformation of some important points are noted. In the ζ plane points on the unit circle are denoted by $u + iv$ or $e^{i\theta}$. Thus the branch point where the crack joins the hole is completely specified by the angle $\theta = \alpha$, and the x coordinate, 1 + a, is specified by $\theta = \theta^*$. Note that α is the upper limit for θ^* if the entire crack is loaded by the yield stress, Y.

for k=1

$$\alpha = \cos^{-1}(-\epsilon) \qquad (17)$$

and

$$\chi = \frac{1}{1-\epsilon}\left\{2\cos\theta + 1 + \epsilon + (1+\cos\theta)\sqrt{(\cos\theta+\epsilon)(1+\cos\theta)} + (1-\cos\theta)\sqrt{(\cos\theta+\epsilon)}\right\} \qquad (18)$$

Equation (18) was solved numerically on a digital computer to determine θ^* for a given 1 + a by using α as the upper limit. For the case of k=2, derivation of an expression similar to (18) proved to be too involved for practical purposes, therefore, θ^* was obtained numerically from the truncated mapping function.

At this point, the right hand side of (15) was expanded into a polynomial as follows

for k=1

$$Z = C\left[s + s^{-1} + 1 + \epsilon + (1+s^{-1})(s^2 + 2\epsilon s + 1)^{1/2} \right] \tag{19}$$

To expand the radical in (19), let $\epsilon = -\cos\alpha$ thus

$$(s^2 + 2\epsilon s + 1)^{1/2} = s\left(1 - \frac{2\cos\alpha}{s} + \frac{1}{s^2}\right)^{1/2}$$

$$= s\left[\left(1 - \frac{e^{i\alpha}}{s}\right)^{1/2} \left(1 - \frac{e^{-i\alpha}}{s}\right)^{1/2} \right] \tag{20}$$

and by applying a binomial expansion to each quantity in brackets in (20), it followed

$$(s^2 + 2\epsilon s + 1)^{1/2} = \left\{ \sum_{n=1}^{\infty} \left[1 - T_n \left(\frac{e^{i\alpha}}{s}\right)^n\right]\left[1 - T_n \left(\frac{e^{-i\alpha}}{s}\right)^n\right] \right\} s$$

$$= s\left[1 + \sum_{n=1}^{\infty} S_n s^{-n} \right] \tag{21}$$

Now, by substituting (21) into (19) and collecting terms, the following infinite polynomial series was obtained.

$$Z = C'\left[s + \sum_{n=1}^{\infty} A_n s^{1-n} \right] \tag{22}$$

where the A_n's are real coefficients and

$$C' = 2C = \frac{2}{1-\epsilon} \tag{23}$$

For k=2 use was made of the expansion for k=1 indicated next.

$$Z = \sqrt{C}\left[s^2 + s^{-2} + 1 + \epsilon + (1+s^{-2})(s^4 + 2\epsilon s^2 + 1)^{1/2} \right]^{1/2} \tag{24}$$

Note that within the braces in (24), the <u>function</u> is identical to that in (19) where s is replaced by s^2. Therefore, the coefficients for that part of (24) are equivalent in form to those in (22), Thus

$$z = \sqrt{c'}\left\{ \zeta^2 + \sum_{n=1}^{\infty} \bar{A}_n \zeta^{2(1-n)} \right\}^{1/2} \qquad (25)$$

The problem then became finding the polynomial whose square yields the polynomial within the braces in (25). This was done by inspection and gave a series of the form:

$$z = \sqrt{c'}\left[\zeta + \sum_{n=1}^{\infty} B_n \zeta^{1-2n} \right] \qquad (26)$$

where the B_n's are real coefficients.

Finally the polynomial representations of the mapping functions were truncated to make possible the solution of the boundary value problem. In truncated form:

for k=1
$$z = \omega_1(\zeta) = c' \sum_{n=0}^{N} A_n \zeta^{1-n}$$

k=2
$$z = \omega_2(\zeta) = \sqrt{c'} \sum_{n=0}^{N} B_n \zeta^{1-2n} \qquad (27)$$

To improve the accuracy of the truncated series, the coefficients, N-2, N-1, and N, were determined in a manner to satisfy the following conditions.

$$dz/d\zeta = \text{actual value} = 0 \quad \text{at} \quad \zeta = 1$$
$$d^2z/d\zeta^2 = \text{"} \quad \text{"} = z_1'' \quad \zeta = 1 \qquad (28)$$
$$\mathcal{I}_m(z) = 0 \quad \theta = \theta^*$$

To determine Z_1'', equations (19) and (24) were differentiated twice and evaluated at $\zeta = 1$. This gave

for k=1

$$z_1'' = C'\left[1 + \frac{\epsilon+3}{2\sqrt{2+\epsilon}}\right] \tag{29}$$

k=2

$$z_1'' = \sqrt{C'}\left[\frac{2\sqrt{2} + (1+3\epsilon)/\sqrt{1+\epsilon}}{3+\epsilon+2\sqrt{2+\epsilon}}\right]$$

In both cases, k=1 and 2, the conditions (28) supplied three linear algebraic equations in the three unknown coefficients, N-2, N-1, and N. The first N-3 coefficients remained those obtained from (22) and (26). The three linear equations are

for k=1

$$(N-3)A_{N-2} + (N-2)A_{N-1} + (N-1)A_N = \sum_{n=0}^{N-3}(1-n)A_n \tag{30}$$

$$(N-3)(N-2)A_{N-2} + (N-2)(N-1)A_{N-1} + (N-1)(N)A_N = \frac{z_1'}{C'} - \sum_{n=0}^{N-3}(1-n)(n)A_n$$

$$\sin\left[(N-3)\theta^*\right]A_{N-2} + \sin\left[(N-2)\theta^*\right]A_{N-1} + \sin\left[(N-1)\theta^*\right]A_N = \sum_{n=0}^{N-3}\sin\left[(1-n)\theta^*\right]A_n$$

and for k=2

$$(2N-5)B_{N-2} + (2N-3)B_{N-1} + (2N-1)B_N = \sum_{n=0}^{N-3}(1-2n)B_n \tag{31}$$

$$(2N-5)(2N-4)B_{N-2} + (2N-3)(2N-2)B_{N-1} + (2N-1)(2N)B_N = \frac{z_1''}{\sqrt{C'}} - \sum_{n=0}^{N-3}(1-2n)(-2n)B_n$$

$$\sin\left[(2N-5)\theta^*\right]B_{N-2} + \sin\left[(2N-3)\theta^*\right]B_{N-1} + \sin\left[(2N-1)\theta^*\right]B_N = \sum_{n=0}^{N-3}\sin\left[(1-2n)\theta^*\right]B_n$$

After the truncated polynomial mapping functions were obtained, the complex boundary value problem was solved using the Muskhelishvili Method.

2.3 Boundary Value Solution

In accordance with Muskhelishvili [6], the complex stress functions were represented in the region exterior to the unit circle in the ζ plane by the following Laurent Series:

$$\varphi(\zeta) = \sum_{-\infty}^{\infty} b_n \zeta^n$$
$$\psi(\zeta) = \sum_{-\infty}^{\infty} c_n \zeta^n \tag{32}$$

where the coefficients are unknown.

For problem B in both cases, k=1 and 2, the stresses vanish as ζ approaches infinity. By applying this condition in conjunction with equations (9) and (32), some of the unknown coefficients were eliminated as follows:

as $\zeta \to \infty$

$$\widehat{ee} = \widehat{\theta\theta} = 0 = 4\,\mathrm{Re}\,\varphi'(\zeta) \tag{33}$$

Differentiating (32) and then substituting into (33) gave

$$\sum_{n=-\infty}^{\infty} n b_n \zeta^{n-1} = 0 \tag{34}$$

For (34) to hold as ζ approaches infinity, the following condition must prevail upon $\varphi'(\zeta)$:

$$n-1 < 0$$
$$n < 1 \tag{35}$$

and thus

$$\varphi'(\zeta) = \sum_{n=-\infty}^{0} n b_n \zeta^{n-1} \tag{36}$$

By remembering that K_B depends upon $\varphi'(\zeta)$ as indicated by equation (10), the coefficient of ζ^0 was neglected and $\varphi(\zeta)$ was written in the following re-indexed form:

$$\varphi(\zeta) = \sum_{n=0}^{\infty} b_n \zeta^{-1-n} \tag{37}$$

Noting that $\varphi''(\zeta) = 0$ as ζ approaches infinity, from the second equation of (9), $\psi'(\zeta)$ was determined to be

$$\psi'(\zeta) = \sum_{n=-\infty}^{0} n c_n \zeta^{n-1} \tag{38}$$

Therefore, in a manner similar to that used for (37), $\psi(\zeta)$ was written in the following re-indexed form:

$$\psi(\zeta) = \sum_{n=0}^{\infty} c_n \zeta^{-1-n} \tag{39}$$

On the unit circle, $\overline{\zeta} = \zeta^{-1}$, and thus (39) gives

$$\overline{\psi(\zeta)} = \sum_{n=0}^{\infty} c_n \zeta^{1+n} \tag{40}$$

The boundary equation, (11), was then employed to determine the remaining unknown coefficients of $\varphi(\zeta)$. Because of the form of $\overline{\psi(\zeta)}$ as given in (40), the resulting coefficients of ζ^j, $j<0$, in (11) produced a set of linear equations, which involve only combinations of the known coefficients of $\omega(\zeta)$,

the known loading function's Fourier coefficients, and the unknown coefficients of $\varphi(\zeta)$. Specifically

$$\varphi(\zeta) + \frac{\omega(\zeta)}{\omega'(\zeta)}\overline{\varphi'(\zeta)} = f_1 + i f_2 \tag{41}$$

To determine $\varphi(\zeta)$ for k=1, it was noted that Y acts normal to the unit circle from $-\theta^*$ to θ^* as shown in Fig. 7. Applying (14) the Fourier Series for the loading function, $f_1 + if_2$, developed as

$$\frac{1}{2\pi}\int_0^{2\pi} Y(\theta)e^{-in\theta}d\theta = \int_0^{\theta^*} Y_1(\theta)e^{-in\theta}d\theta + \int_{\theta^*}^{2\pi-\theta^*} Y_2(\theta)e^{-in\theta}d\theta + \int_{2\pi-\theta^*}^{2\pi} Y_3(\theta)e^{-in\theta}d\theta \tag{42}$$

ξ times factor $\frac{1}{2\pi}$

Now using

$$Y(\theta) = Y\omega_1(\zeta) = c'Y\sum_{n=0}^{N} A_n \zeta^{1-n} = c'Y\sum_{n=0}^{N} A_n e^{(1-n)i\theta} \tag{43}$$

it followed that

$$\begin{aligned} Y_1(\theta) &= c'Y\sum_{j=0}^{N} A_j e^{(1-j)i\theta} \\ Y_2(\theta) &= c'Y\sum_{j=0}^{N} A_j e^{(1-j)i\theta^*} \\ Y_3(\theta) &= c'Y\sum_{j=0}^{N} A_j e^{(1-j)i\theta} \end{aligned} \tag{44}$$

By substituting (44) back into (42), the integration yielded

$$\sum_{n=-\infty}^{\infty} d_n \zeta^n = \sum_{n=-\infty}^{\infty}\left\{\frac{c'Y}{\pi}\left[\sum_{j=0}^{N} A_j\left(\frac{\sin(1-j-n)\theta^*}{(1-j-n)} - e^{(1-j)i\theta^*}\frac{\sin n\theta^*}{n}\right)\right]\right\}\zeta^n \tag{45}$$

where from (28) and (43)

$$c'\sum_{j=0}^{N} A_j e^{(1-j)i\theta^*} = c'\sum_{j=0}^{N} A_j \cos(1-j)\theta^* \tag{46}$$

since the imaginary part of $\omega_1(\zeta)$ was forced to zero at $\Theta = \Theta^*$.

Next using (27)

$$\omega_1(\zeta) = c' \sum_{n=0}^{N} A_n \zeta^{1-n}$$

thus

$$\overline{\omega_1'(\zeta)} = c' \sum_{n=0}^{N} (1-n) A_n \zeta^{n} \tag{47}$$

Using (37)

$$\varphi(\zeta) = \sum_{n=0}^{\infty} b_n \zeta^{-1-n}$$

thus

$$\overline{\varphi'(\zeta)} = \sum_{n=0}^{\infty} (-1-n) b_n \zeta^{2+n} \tag{48}$$

Finally applying (27), (37), (45), (47) and (48) to equation (41) resulted in

$$\sum_{n=0}^{\infty} b_n \zeta^{-1-n} + \frac{c' \sum_{n=0}^{N} A_n \zeta^{1-n}}{c' \sum_{n=0}^{N} (1-n) A_n \zeta^{n}} \sum_{n=0}^{\infty} (-1-n) b_n \zeta^{2+n} = \sum_{n=1}^{\infty} d_n \zeta^{-n} \tag{49}$$

A study of the above expanded series multiplications revealed that N mapping terms yielded a set of linear algebraic equations for b_o to b_M where $M = N - 4$. For $n > M$, b_n was obtained from the reduced form of (41):

$$\sum_{n=M+1}^{\infty} b_n \zeta^{-1-n} = \sum_{n=M+2}^{\infty} d_n \zeta^{-n} \tag{50}$$

Multiplying out the series in (49) yielded

$$\frac{\sum_{n=0}^{N} A_n \zeta^{1-n}}{\sum_{n=0}^{N} (1-n) A_n \zeta^{n}} \sum_{n=0}^{\infty} (-1-n) b_n \zeta^{2+n} = \sum_{n=0}^{M} \frac{1}{b_n} \zeta^{n} \sum_{n=0}^{N} A_n \zeta^{1-n} \sum_{n=0}^{\infty} (-1-n) b_n \zeta^{2+n}$$

$$= \sum_{n=0}^{\infty} d_n \zeta^{n+1-N} \sum_{n=0}^{\infty} (-1-n) b_n \zeta^{2+n} \tag{51}$$

It was noted that only part of the $\sum_{n=0}^{\infty} a_n \zeta^{n+1-N}$ affects the ζ^j , $j<0$, terms of (49). Therefore it was re-written in the following way:

$$\sum_{n=0}^{M} a_n \zeta^{n+1-N} = \sum_{n=0}^{M} g_n \zeta^{-n-s} \tag{52}$$

where $g_n = s_{M-n}$.

Substituting (52) back into (51), and then back into (49), yielded the following set of linear equations for b_n:

Index, p, varies from 0 to M in

$$b_p + \sum_{n=0}^{M-P} (-1-n) g_{P+n} b_n = d_{P+1} \tag{53}$$

Equations, (53) when solved simultaneously, determined the first 0 to M coefficients of $\varphi(\zeta)$. Equation (50) yielded the remaining, n > M, coefficients. The third condition on the truncated mapping function as expressed by (28), insures that the imaginary part of $\omega(\zeta)$ equals zero at $\theta = \theta^*$. Inserting this fact as equation (46) into (45) enabled the convergence of d_n to zero as n approaches infinity to be shown. See Appendix B. Therefore, in conjunction with (50), the numerical convergence of $\varphi(\zeta)$ and more important $\varphi'(\zeta)$ was assured.

Numerical tests were run to learn the effect of N on the n-th coefficient, d_n. These results are reported later and were used to determine the number of terms in $\varphi(\zeta)$ required to achieve the desired accuracy. Thus $\varphi(\zeta)$ was computed by two sums:

$$\varphi(\zeta) = \sum_{n=0}^{M} b_n \zeta^{-1-n} + \sum_{n=M+1}^{Q} b_n \zeta^{-1-n} \tag{54}$$

For k=2, $\varphi(\zeta)$ was determined in a fashion similar to that for k=1 with the following modifications. The twin crack problem is symmetric in both loading and geometry with respect to the coordinate axes. Therefore, the problem was modified to the linear superposition of the twin crack with plastic loading only on the right hand crack tip, Problem C, plus the twin crack with plastic loading only on the left hand crack tip, Problem D, as illustrated in Fig. 8. It was then noted that D is exactly the same as C where the coordinate axes are rotated π radians. For that amount of rotation, Muskhelishvili [6] shows that the corresponding functional transformation is

$$\varphi_D'(\zeta_D) = \varphi_C'(-\zeta_D) \tag{55}$$

Thus, for application to the solution of the stress intensity factor as indicated by (10)

$$\begin{aligned} \varphi'(\zeta) &= \varphi_C'(\zeta) + \varphi_D'(\zeta_D) \\ &= \varphi_C'(\zeta) + \varphi_C'(-\zeta_D) \end{aligned} \tag{56}$$

and the problem is solved by determining the coefficients of $\varphi_c(\zeta)$.

Comparison of the ζ planes for k=1 and k=2 as shown for C in Fig. 9, revealed that the Fourier Series for the loading function of C is the same as that for k=1 where the only difference comes from the twin crack mapping function. Thus from

$$Y(\theta) = Y\omega_2(\zeta) = \sqrt{c'}\, Y \sum_{n=0}^{N} B_n e^{(1-2n)i\theta} \qquad (57)$$

where the power (1-2n) replaces (1-n) in (43), the Fourier Series for C is obtained from (45) by replacing j with 2j:

$$\sum_{n=-\infty}^{\infty} d_n \zeta^n = \sum_{n=-\infty}^{\infty} \left\{ \frac{\sqrt{c'}Y}{\chi} \left[\sum_{j=0}^{N} B_j \left(\frac{\sin(1-2j-n)\theta^*}{(1-2j-n)} - e^{(1-2j)i\theta^*} \frac{\sin n\theta^*}{n} \right) \right] \right\} \zeta^n \qquad (58)$$

where from (28) and (57)

$$\sqrt{c'} \sum_{j=0}^{N} B_j e^{(1-2j)i\theta^*} = \sqrt{c'} \sum_{j=0}^{N} B_j \cos(1-2j)\theta^* \qquad (59)$$

since the imaginary part of $\omega_2(\zeta)$ was forced to zero at $\theta = \theta^*$.

Next using (27)

$$\omega_2(\zeta) = \sqrt{c'} \sum_{n=0}^{N} B_n \zeta^{1-2n}$$

thus

$$\overline{\omega_2'(\zeta)} = \sqrt{c'} \sum_{n=0}^{N} (1-2n) B_n \zeta^{2n} \qquad (60)$$

Using (37)

$$\varphi_c(\zeta) = \sum_{n=0}^{\infty} b_n \zeta^{-1-n}$$

thus

$$\overline{\varphi_c'(\zeta)} = \sum_{n=0}^{\infty} (-1-n)\, \zeta^{2+n} \qquad (61)$$

Finally applying (27), (37), (58), (60) and (61) to equation (41) resulted in

$$\sum_{n=0}^{\infty} b_n \zeta^{-1-n} + \frac{\sqrt{c'} \sum_{n=0}^{N} B_n \zeta^{1-2n}}{\sqrt{c'} \sum_{n=0}^{N} (1-2n) B_n \zeta^{2n}} \sum_{n=0}^{\infty} (1-n) b_n \zeta^{2+n} = \sum_{n=1}^{\infty} d_n \zeta^{-n} \qquad (62)$$

Expansion and multiplication of the series in (62) revealed two independent sets of linear algebraic equations for the even and odd b_n's. For odd n's, i.e., $b_1 \zeta^{-2} + b_3 \zeta^{-4} + \ldots$, the coefficients are all identically equal to zero. For the even n's, N terms in the mapping function yielded a set of linear algebraic equations for b_0 to b_{2M} where $M = N - 2$. For $n > 2M$, b_n was obtained from the reduced form of (41) as indicated by (50):

$$\sum_{n=2M+1}^{\infty} b_n \zeta^{-1-n} = \sum_{n=2M+2}^{\infty} d_n \zeta^{-n} \qquad (50)$$

where all d_n's, n is even, are identically equal to zero.

Multiplying out the series in (62) yielded

$$\frac{\sum_{n=0}^{N} B_n \zeta^{1-2n}}{\sum_{n=0}^{N} (1-2n) B_n \zeta^{2n}} \sum_{n=0}^{\infty} (-1-n) b_n \zeta^{2+n} = \sum_{n=0}^{M} f_n \zeta^{2n} \sum_{n=0}^{N} B_n \zeta^{1-2n} \sum_{n=0}^{\infty} (-1-n) b_n \zeta^{2+n}$$

$$= \sum_{n=0}^{\infty} g_n \zeta^{2n+1-2N} \sum_{n=0}^{\infty} (-1-n) b_n \zeta^{2+n} \qquad (63)$$

It was noted that only part of the $\sum_{n=0}^{\infty} g_n \zeta^{2n+1-2N}$ affects the ζ^j , $j < 0$, terms of (62). Therefore it was rewritten in the following way:

$$\sum_{n=0}^{M} g_n \zeta^{2n+1-2N} = \sum_{n=0}^{M} q_n \zeta^{-3-2n} \qquad (64)$$

where $g_n = q_{M-n}$.

Substituting (64) back into (63), and then back into (62), yielded the following set of linear equations for b_n where n is even:

Index p varies from 0 to M in

$$b_{2p} + \sum_{n=0}^{M-p} (-1-2n)\, g_{p+n}\, b_{2n} = d_{2p+1} \qquad (65)$$

Equations (65), when solved simultaneously, determined the first 0 to 2M coefficient of $\varphi_c(\zeta)$. Equation (50) yielded the remaining, $n > 2M$, coefficients. The convergence properties for d_n shown for k=1 in Appendix B also apply to k=2. Therefore, the numerical convergence of $\varphi_c(\zeta)$ and $\varphi_c'(\zeta)$ was assured. Convergence studies for the twin crack are reported later, which determined Q for the number of mapping terms, N, to yield the desired accuracy of $\varphi_c(\zeta)$. Thus $\varphi_c(\zeta)$ was computed by two sums:

$$\varphi_c(\zeta) = \sum_{n=0}^{M} b_{2n} \zeta^{-1-2n} + \sum_{n=M+1}^{Q} b_{2n} \zeta^{-1-2n} \qquad (66)$$

2.4 Stress Intensity Factors

The stress functions for k=1 and 2 were found in the previous section and shown as

$$\text{for } k=1 \qquad \varphi(\zeta) = \sum_{n=0}^{Q} b_n \zeta^{-1-n}$$

$$k=2 \qquad \varphi_c(\zeta) = \sum_{n=0}^{Q} b_{2n} \zeta^{-1-2n} \tag{67}$$

These were applied to (10) to determine the stress intensity factor at the crack tip, $\eta=1$. The quantity $\omega'(\zeta)$ was written in the following alternate form to ease the solution of (10). Since $\omega'(\zeta)$ is zero when $\zeta=1$, it can be written as

$$\omega'(\zeta) = (\zeta-1)\, g(\zeta) \tag{68}$$

where $g(\zeta)$ is a polynomial whose coefficients are chosen such that the roots of $g(\zeta)=0$ fall inside the unit circle. Differentiating (68) yields

$$\omega''(\zeta) = (\zeta-1)\, g'(\zeta) + g(\zeta) \tag{69}$$

Then solving for $g(\zeta)$ in (69) and substituting back into (68) reveals

$$\omega'(\zeta) = (\zeta-1)\left[\omega''(\zeta) - (\zeta-1)\, g'(\zeta)\right] \tag{70}$$

For a crack tip at $\zeta=\eta=1$, $\omega(\zeta)$ was expanded about $\zeta=1$ in equation (10); then (70) was applied to give

$$K_B = 2\sqrt{2}\lim_{\zeta\to 1}\left\{\left[\omega(\zeta)-\frac{(\zeta-1)}{1!}\omega'(\zeta)+\frac{(\zeta-1)^2}{2!}\omega''(\zeta)+\ldots-\omega(1)\right]^{\frac{1}{2}}\frac{\varphi'(\zeta)}{(\zeta-1)\omega'(\zeta)}\right.$$

$$\left. = 2\sqrt{2}\lim_{\zeta\to 1}\left\{\frac{(\zeta-1)\sqrt{\omega''(\zeta)}}{\sqrt{2}}\quad\frac{\varphi'(\zeta)}{(\zeta-1)\omega'(\zeta)}\right\}\right.$$

thus

$$K_B = 2\,\varphi'(1)\Big/\sqrt{z_1''} \tag{71}$$

By using (29) and (67) in conjunction with (71), the stress intensity factor at the crack tip for k=1 was determined to be

$$K_{B1} = \frac{2}{\sqrt{z_1''}}\sum_{n=0}^{Q}(-1-n)b_n \tag{72}$$

For k=2, $\varphi'(1)$ was found from $\varphi_c(\zeta)$ by applying equation (56); then substituted into (71) to yield

$$K_{B2} = \frac{4}{\sqrt{z_1''}}\sum_{n=0}^{Q}(-1-2n)b_{2n} \tag{73}$$

Note that the stress intensity factors from (72) and (73) are normalized with respect to Y, which multiplies each Fourier Series term of (45) and (58).

2.5 Plastic Enclave Sizes

The preceding analysis and associated computer programs determined K_{Bk} for k=1 and 2. For different loadings at infinity and various L/R ratios, these stress intensity factors were used to determine the plastic enclave sizes according to the condition of equation (7) by the following method. Refer to Fig. 7.

1.) For both k=1 and 2, K_B was obtained for various values of W/L and L/R ratios. These values are tabulated in Tables 4 and 6 and are plotted on Figs. 10, 11, and 12. The actual K_B values are negative, but they are plotted positive for graphical convenience. The stress intensity factors, K_A, were taken from reference [7] and tabulated in Table 7. They are also shown on Figs. 10, 11, and 12.

2.) The desired results are to yield W/L for given a/R and σ_∞/Y ratios. Therefore the following notation is adopted.

$$\eta = W/L \quad , \quad \chi = a/R \tag{74}$$

Since the K_{Bk}'s were computed based upon the crack, a, plus enclave, W, the relationship between a/R and L/R was needed for a specific W/L. Thus

$$\frac{L}{R} = \frac{a+w}{R} = \frac{a}{R} + \frac{w}{L}\frac{L}{R}$$

$$\frac{L}{R} = \frac{x}{1-y} \qquad (75)$$

The parameter, L/R, is tabulated for incremented values of y between .05 and .8 and x between .5 and 10 in Table 1.

3.) For the x's and y's chosen, the ratios of stress intensity factors, K_{Bk}/K_{Ak}, were obtained from Figs. 10, 11, and 12 at the corresponding L/R's. Taking into account the normalizing of K_{Bk} with respect to Y, the stress ratios at any a/R$\longleftrightarrow$L/R were determined from the plasticity condition on the stress intensity factors. Namely

$$K_{Ak}\,\sigma_\infty + K_{Bk}\,Y = 0$$

thus

$$\sigma_\infty/Y = -K_{Bk}/K_{Ak} \qquad (76)$$

where K_{Bk} is a negative number. In this fashion Table 8 was constructed and the plots of W/L versus σ_∞/Y for various a/R values were obtained and given in Figs. 13 and 14. These plots represent the plastic enclave solution based upon the Dugdale Model.

III. Results of Analytical Analysis

The discussion of analytical results is presented in two parts. First the convergence of data for K_B as obtained from the computer is evaluated. The accuracy of these results is estimated. Second the magnitudes of the resulting plastic enclaves are considered with respect to the problem's dimensions.

As noted in the analytical development, the mapping polynomial was truncated at N terms, and the stress function was approximated by a finite series of Q terms. It remained to determine the influence of these numerical approximations on the accuracy of the results. The stress function, $\varphi(s)$, was the quantity initially affected. However, the stress intensity factors, which are directly related to the stress function's first derivative by (10), were chosen to measure the convergence of solution because of their close relation to the plastic enclave sizes.

For k=1 the effect of the mapping function truncation was tested by varying N while fixing Q at 99. Noting that M is a direct reflection of N since M = N - 4, the results of this test are shown in Table 2a. The maximum storage capacity of the digital computer limited the unsegmented program to M = 24. For the trial of M = 46 a segmented modification of the original program

was written. The rate of convergence for the mapping polynomial decreases as L/R decreases. Thus a crack length, L/R = 2, was chosen to test the poorest condition of $\omega(\zeta)$. One can see that in the range of M from 15 to 46, the fluctuations in K are of the order 2 out of 270 for W/L = 0.05 and 5 out of 680 for W/L = 0.30 for less than a 1% deviation.

The effect of the number of terms in the stress function series was tested by varying Q such that the terms added to the initial M, i.e., Q-M, ranged from 0 to 275 while M was held constant at 22. Table 2b indicates the trend evident from this study. Variations on L/R and W/L can be seen to have had no significant effect on the convergence of K_B. In all cases the maximum deviation between any two data are less than 2%. Therefore, the results from the program for k=1 are assumed to converge within 2% of the true value.

As a final check on the program, the results for k=1, L/R = 10, M = 24, and Q = 99 were compared to the closed form solution for the stress intensity factor at the crack tip where normal stresses act on the open surface of an internal crack. The solution is given by Paris and Sih [1] for the case where R = o, which corresponds to L/R approaching infinity in this plastic enclave problem. Thus the solution for a large L/R was

was compared to the computer program's solution for L/R = 10. The results are reported in Table 3 and are comparable as an approximate check.

Therefore, all of the stress intensity factors plotted in Fig. 10 and tabulated in Table 4 were obtained with M = 24 and Q = 99. These are assumed to be accurate to within 2% of the true values.

For k=2, the effect of the mapping function truncation and the stress function's finite polynomial approximation on the convergence of the stress intensity factors was studied in the same manner as previously indicated for k=1. Once again the deviation between converging results is less than 2% as observable in Table 5. Thus all the stress intensity factors plotted in Figs. 11 and 12, and recorded in Table 6 were obtained with M = 24 and Q = 99. It is assumed that this data is also accurate to within 2% of the true values.

Plastic enclave sizes for k=1 and 2 are tabulated in Table 8 and represented in Figs. 13 and 14 respectively. To convert the ratio of W/L to W for a given a/R, use

$$w = {}^{ya}\!/_{(1-y)} \qquad (77)$$

For k=1, sufficient σ_∞ or L/R ratios is expected to cause plastic yielding along the circular cavity opposite the crack. This condition was not included

in the plastic enclave model. Therefore, only a sample data range is presented to demonstrate the method of determining enclave sizes. The range in which the enclave model applies could be found by first computing the stress function at $z = -1$, $\zeta = -1$, then applying them to equations (9) to determine the stresses. The parameters σ_∞/Y and L/R which first create stresses large enough to cause yielding based upon some type of yield criterion, i.e., Tresca or Von Mises, form the limiting boundary on the Dugdale Model's application to the enclave solution. The defining of this applicable region was not the object of this thesis and is left open for further investigation.

When k=2, the Dugdale plastic enclave model more closely approximates the physical problem than it does for k=1 over the full range of loading and geometry parameters. Therefore, the complete plastic enclave solution is presented for all $a/R > 0.5$. As a/R approaches infinity, the solution is seen to approach the plastic zone solution by Dugdale [3] for internal straight cracks in elastic plates under tension. For $a/R < 0.5$, the physical problem approaches the determination of plastic enclaves adjacent to a circular hole in an infinite plate under tension. For this lower range of a/R reference [7] presented no data for K_A because of

the inherent poor convergence of the numerical system of equations which determine them. Thus, the twin numerical plastic enclave solution was limited to $a/R \geq 0.5$. However, the numerical methods for both K_A and K_B, and thus for W/L, are applicable and easily extended to lower ranges of a/R with the aid of a computer with large storage capacity.

The Dugdale internal crack solution can be seen in Fig. 14 to approximate that for the twin crack situation only for various ranges of a/R depending upon the applied load. The largest variation comes at $\sigma_\infty / Y = 0.5$ where, for example, an internal straight crack, which is three inches in length, possesses a 0.6 inch plastic enclave at each crack tip. When a one inch circular hole is introduced at the crack center, the enclave size increases to 0.75 inches. This represents a 25% increase over the straight crack estimation.

IV. Conclusions and Possible Future Work

The analytical method and numerical solution presented in the estimation of plastic enclave sizes for cracks emanating from a circular void within an elastic plate under tension can be extended to handle other configurations of loading and geometry. For example, a solution for the representative plastic zone lengths of the same geometrical problem subjected to a cylindrical bending load at infinity can be obtained by the appropriate changes in the boundary conditions for solution of the elastic stress intensity factors resulting from external loading. Variations in the problem geometry such as internal voids of elliptical or any arbitrary shape can be coped with providing it can be mapped to a unit circle in a complex plane by a truncated polynomial. Plastic enclaves at the tips of edge cracks in various shaped plates can also be estimated provided they meet the same mapping requirement. The remainder of the analysis follows that presented for circular voids.

For each new geometric and loading configuration, the applicability of Dugdale's plastic zone model must be evaluated with respect to the physical problem. Any enclave model, which will approximate the mode of crack deformation and linearize the plasticity effect,

can be incorporated into the boundary value problem and solved by the numerical techniques presented. E. J. Brown [8] suggests a model which employs a thin strip along the crack line to represent the plastic yield zone for a plane problem with arbitrary loads in the plane of the plate. The material in the yielded zone is then removed and the crack allowed to extend to the limits of the yield zone. The resulting plastic stresses at the yield zone's edge are applied as surface tractions along the crack extension. This approach is similar to Dugdale's, however, this model includes the variations in normal tractions and also the shear tractions which result from plastic yielding.

Rosenfield, Dai, and Hahn [4] vary the normal plastic stresses in the Dugdale model to account for strain hardening effects in the crack tip region. Their modifications enable them to calculate crack propagation parameters which more closely approximate experimental results at high external load to yield ratios, than does the unmodified Dugdale model. This type of variation is easily incorporated into the thesis method by proper adjustment of the loading functions over the enclave surface.

In the circular void with emanating cracks problem, the analytical results were checked against limiting solutions found in the literature. However, a direct experimental verification of the analytical solution is proposed which employs reflective photoelastic techniques. The photoelastic coating is applied to the specimen, and then the voids plus cracks are introduced to the specimen-coating combination to assure the proper matching of boundary conditions in the specimen and photoelastic coating material. In conjunction with a method for separation of stresses or strains, i.e., oblique incidence reflective photoelastic techniques or a shear difference method, the normal reflective technique will yield the principal stresses and/or strains at the plastic enclave region preceding the crack tip. Application of a plastic yield criterion, i.e., Tresca, Von-Mises or an arbitrary establishment of a principal plastic strain threshold, will then determine a representative plastic enclave length. These measurements will provide a direct experimental check of analytical results. The photoelastic method can be employed to check any plastic enclave problem within the physical limitations of the coating material and bonding substance.

V. Appendices

Appendix A Mapping Functions

Refer to Fig. 7

for k=1

$$z = \omega_1(\zeta) = C\left[\zeta + \zeta^{-1} + 1 + \epsilon + (1+\zeta^{-1})(\zeta^2 + 2\epsilon\zeta + 1)^{1/2}\right] \quad (a)$$

where

$$\epsilon = 2\left[\frac{L}{L+2}\right]^2 - 1 \quad (b)$$

A1.) Find the limiting values of ϵ :

$$\lim_{L\to\infty} \epsilon = \lim_{L\to\infty} 2\left[\frac{1}{1+\frac{2}{\infty}L}\right]^2 - 1 = 2 - 1 = +1$$

$$\lim_{L\to 0} \epsilon = \lim_{L\to 0} 2\left[\frac{1}{1+\frac{2}{L}\cdot 0}\right]^2 - 1 = 0 - 1 = -1$$

A 2.) Find C such that R = 1 in the z plane

put $\zeta = 1$ into (a)

$$z = R + L = C\left[(3+\epsilon) + 2\sqrt{2+\epsilon}\right]$$

for R = 1 and ϵ from (b)

$$1 + L = C\left[3 + \left[2\left(\frac{L}{L+2}\right)^2 - 1\right] + 2\sqrt{2}\left[1 + 2\left(\frac{L}{L+2}\right)^2 - 1\right]^{1/2}\right]$$

$$\simeq C\left[2\left(1 + \frac{L}{L+2}\right)^2\right]$$

$$\therefore \quad C = (1+L) \Big/ 2\left[1 + \frac{L}{L+2}\right]^2 = \frac{(L+2)^2}{8(L+1)}$$

$$= \frac{(L+2)^2}{2L^2 + 8L + 8 - 2L^2} = \frac{1}{2 - 2\left(\frac{L^2}{(L+2)^2}\right)}$$

$$= \frac{1}{1 - \left[2\left(\frac{L}{L+2}\right)^2 - 1\right]} = \frac{1}{1-\epsilon} \quad (c)$$

A 3.) To Find α i.e., Branch Point

use (a) where z = 1

$$f = e^{i\theta} = \cos\theta + i\sin\theta$$

at the branch point $\sqrt{\text{term}}$ in (a) = 0

$$\theta = \alpha$$

and

$$1 = \frac{1}{1-\epsilon}\left\{\cos\theta + i\sin\theta + \cos\theta - i\sin\theta + 1 + \epsilon\right\}$$

$$1-\epsilon = 2\cos\theta + 1 + \epsilon$$

$$2\cos\theta = 2\cos\alpha = -2\epsilon$$

$$\therefore \alpha = \cos^{-1}(-\epsilon) \qquad (d)$$

A 4.) Find $X(\theta)$:

1. substitute $\zeta = u + iv$ into (a)

$$z = C\left[(u+iv) + (u+iv)^{-1} + 1 + \epsilon + \left\{1+(u+iv)^{-1}\right\}\{c + i\,d\}\right] \qquad (e)$$

$$= C\left[X + i\,Y\right] \qquad (f)$$

Real Part:

$$X = u + \frac{u}{u^2+v^2} + (1+\epsilon) + \left[1 + \frac{u}{u^2+v^2}\right]c + \left[\frac{v}{u^2+v^2}\right]d \qquad (g)$$

where

$$c = \mathrm{Re}\,(\zeta^2 + 2\epsilon\zeta + 1)^{1/2} \quad ; \quad d = \mathrm{Im}\,(\zeta^2 + 2\epsilon\zeta + 1)^{1/2}$$

$$\zeta^2 + 2\epsilon\zeta + 1 = \left[u^2 - v^2 + 2\epsilon u + 1\right] + \left[2uv + 2\epsilon v\right] i$$

$$= a + b\,i = \rho_0\, e^{i\gamma}$$

$$\rho_0^2 = a^2 + b^2 = u^4 + 4\epsilon u^3 + (2v^2 + 2 + 4\epsilon)u^2 + (4\epsilon v^2 + 4\epsilon)u$$

$$+1 + (4\epsilon^2 - 2)v^2 + v^4 \qquad (h)$$

$$\gamma = \tan^{-1}\left(\frac{b}{a}\right) = \tan^{-1}\left[\frac{2uv + 2\epsilon v}{u^2 - v^2 + 2\epsilon u + 1}\right]$$

now $$\left[a+bi\right]^{1/2} = c + di = \rho_0^{1/2}\, e^{i\frac{\gamma}{2} + n\pi}$$

for n = 0

$$c^2 + d^2 = \rho_0$$

$$\tan\frac{\gamma}{2} = \frac{d}{c}$$

solve for c & d

$$c = \left[\rho_0 \cos^2\frac{\gamma}{2}\right]^{1/2} \qquad (i)$$

$$d = \left[\rho_0 \cos^2\frac{\gamma}{2}\right]^{1/2} \tan\frac{\gamma}{2}$$

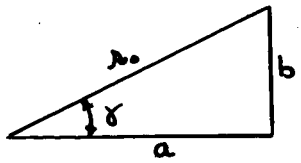

$$\tan\frac{\gamma}{2} = \left[\frac{(s-a)(s-r_o)}{s(s-b)}\right]^{1/2}$$

where $s = 1/2\,(a+b+r_o)$

reduces to

$$\tan\frac{\gamma}{2} = \left[\frac{a\sqrt{a^2+b^2} - a^2}{a\sqrt{a^2+b^2} + a^2}\right]^{1/2}$$

and

$$\cos^2\frac{\gamma}{2} = \left[\frac{s(s-b)}{a\,r_o}\right] = \frac{1}{2} + a/2\sqrt{a^2+b^2}$$

substitute back using $r_o = \sqrt{a^2 + b^2}$ and obtain from (i)

$$c = \left(\frac{r_o + a}{2}\right)^{1/2}$$

$$d = \left(\frac{r_o - a}{2}\right)^{1/2}$$

2. use condition on unit circle

i.e.:

$$u^2 + v^2 = 1$$

$$\therefore\ v^2 = 1 - u^2 \quad ; \quad v = \sqrt{1-u^2}$$

$$v^4 = 1 - 2u^2 + u^4$$

subst. in for r_o^2 in (h)

$$r_o^2 = 4(u^2 + 2\epsilon u + \epsilon^2)$$

$$\therefore\ r_o = 2(u+\epsilon)$$

similarly for a

$$a = 2u(u+\epsilon)$$

$$c = \left[(u+\epsilon)(1+u)\right]^{1/2} \qquad (j)$$

$$d = \left[(u+\epsilon)(1-u)\right]^{1/2}$$

substituting (j) and unit circle condition back into (g)

$$X = 2u + (1+\epsilon) + (1+u)\sqrt{(u+\epsilon)(1+u)} + (1-u)\sqrt{(u+\epsilon)} \qquad (k)$$

3. Note that on unit circle $u = \cos\theta$
and multiplying X by C as indicated in (f)
obtain:

$$C = \frac{1}{1-\epsilon}$$

$$\chi(\theta) = \frac{1}{1-\epsilon}\left\{2\cos\theta + (1+\epsilon) + (1+\cos\theta)\sqrt{(\cos\theta+\epsilon)(1+\cos\theta)} + (1-\cos\theta)\sqrt{(\cos\theta+\epsilon)}\right\} \qquad (l)$$

Appendix B Convergence of the Loading Function's Complex Fourier Series

for k=1

from equation (45)

$$\sum_{-\infty}^{\infty} d_n \rho^n = \sum_{n=-\infty}^{\infty} \left\{ \frac{c'\gamma}{\pi} \left[\sum_{j=0}^{N} A_j \left(\frac{\sin(1-j-n)\theta^*}{(1-j-n)} - e^{(1-j)i\theta^*} \frac{\sin n\theta^*}{n} \right) \right] \right\} \rho^n \qquad (m)$$

where from (46)

$$c' \sum_{j=0}^{N} A_j e^{(1-j)i\theta^*} = c' \sum_{j=0}^{N} A_j \cos(1-j)\theta^* \qquad (n)$$

substituting (n) into the quantity within braces in (m) yields

$$\{\ \} = \left\{ \frac{c'\gamma}{\pi} \left[\sum_{j=0}^{N} A_j \left(\frac{\sin(1-j-n)\theta^*}{(1-j-n)} - \frac{\cos(1-j)\theta^* \sin n\theta^*}{n} \right) \right] \right\} \qquad (o)$$

expanding $\sin(1-j-n)\theta^*$ into $\sin(1-j)\theta^* \cos\theta^* - \sin\theta^* \cos(1-j)\theta^*$ and substituing back into (o) and then (m)

$$d_n = \frac{c'\gamma}{\pi} \sum_{j=0}^{N} A_j \left(\frac{\sin(1-j)\theta^* \cos n\theta^*}{(1-j-n)} - \frac{(1-j)\cos(1-j)\theta^* \sin n\theta^*}{n(1-j-n)} \right) \qquad (p)$$

For large negative n:

$$1-j-n \cong n$$

Thus for (p)

$$d_n = \frac{c'\gamma}{\pi} \left\{ \sum_{j=0}^{N} A_j \sin(1-j)\theta^* \frac{\cos n\theta^*}{n} + \sum_{j=0}^{N} A_j (1-j) \cos(1-j)\theta^* \frac{\sin n\theta^*}{n^2} \right\} \qquad (q)$$

Noting from condition three in equation (28), $\mathcal{I}_m(z)=0$ at $\theta=\theta^*$

Thus

$$C' \sum_{j=0}^{N} A_j \sin(1-j)\theta^* = 0 \qquad (r)$$

using (r) take limit of d_n as $n \to -\infty$

$$\lim_{n\to-\infty} d_n = \frac{Y}{\pi}\left\{ C' \sum_{j=0}^{N} A_j \sin(1-j)\theta^* \frac{\cos n\theta^*}{n} + C' \sum_{j=0}^{N} A_j (1-j)\cos(1-j)\theta^* \frac{\sin n\theta^*}{n^2} \right\} \qquad (s)$$

$$= 0$$

Based on (50), (s) insures the convergence of $\varphi(\xi)$ as $n \to -\infty$. However, K_B depends upon $\varphi'(\xi)$ as indicated by (10), therefore, the convergenec of $\varphi'(\xi)$ for large negative n is desired. Differentiating (50) yields the form of the coefficient of $\varphi'(\xi)$ as $n \to -\infty$

$$\lim_{n\to-\infty} n d_n = \frac{Y}{\pi}\left\{ C' \sum_{j=0}^{N} A_j \sin(1-j)\theta^* \cos n\theta^* + C' \sum_{j=0}^{N} A_j (1-j)\cos(1-j)\theta^* \frac{\sin n\theta^*}{n} \right\}$$

$$= 0 \qquad (t)$$

For k=2, the Fourier Series is given by (58), which is similar to that for k=1 where j is replaced by 2j. Thus the proof of convergence for $\varphi(\xi)$ and $\varphi'(\xi)$ is the same as that above for k=1.

Appendix C Application to Computer Solution

C 1.) General Notes:

Computer programs were written for both the single and twin crack problems with slight modifications employed to make the convergence studies. A detailed description of the program for k=2 is presented here. The one for k=1 is very similar, with the major change arising from the difference in mapping functions. It will be kept on file by the author for five years from the date of this thesis. The programs were written in the Lewiz algebraic programming language and operated on the Lehigh University GE-225 Computer.

The various parts of the program for k=2 can be associated to the analytical development of the plastic enclave sizes by consulting the following flow chart and sample listing in conjunction with the referenced program notation.

C 2.) Program Notation:

The following list identifies the computer program variables corresponding to the main variables in the analytical development. Where applicable the specific equation number is given which refers to the most important relationship in the solution invloving the variable. The remaining variables, not listed, are either dummy indexes or variables used in loops to determine the main ones as listed.

Computer Variable	Problem Variable	Equation or Figure
ADD	$Q-M$	(66)
A2D1	Z_1''	(29)
BB	b_{2n}	(66)
CL	L/R	Fig. 7
COEF	$\sqrt{C'}$	(23)
CON	B_{N-2}, B_{N-1}, B_N (coef.)	(31)
COR	$1+a$	Fig. 7
DD	d_n	(58)
E	ϵ	(16)
EP	B_n	(27)
FF	ρ_{fR}	(63)
GG	g_n	(64)
G1	$M+1$	(66)
G2	$M+2$	
G3	$M+3$	
G4	N	(27)

HH	coeff. of b	(65)
IMAG	$\mathrm{Im.}(z)$	(28)
KTP	K_B	(73)
LAMBDA	λ	(16)
LNH	$1+a$	Fig. 7
MF	$Q+1$	
NBAR	N	(27)
NSTAR	M	(66)
O	Θ^*	Fig. 7
P	P	(65)
PHIPRIME1	$\varphi'(1)$	(71), (72)
PIP	$\varphi'(1)$ sum M+1 to Q	
RPE	w numerical	Fig. 7
RWL	w/L numerical	Fig. 7
T	T	(21)
V, VV1, VV2, VV3	B_{N-2}, B_{N-1}, B_N (coef.)	(31)
WL	w/L	Fig. 7
ZMI	$\omega(-1)$	(27)
ZPRIME1	$\omega'(1)$	
ZPI	$\omega(1)$	
Z2PRIME1	$\omega''(1)$	

C 3.) Input:

The input was punched on cards following the Lewiz format in the following order:

1st	number of L/R values
2nd	number of N values
3rd	Q + 1
4th	initial value of W/L
5th	final value of W/L
6th	increment size of W/L
7th	L/R values
8th	N values

C 4.) Sample Listing and Output:

As follows -

C 5.) FLOW CHART FOR PLASTIC ENCLAVE PROGRAM

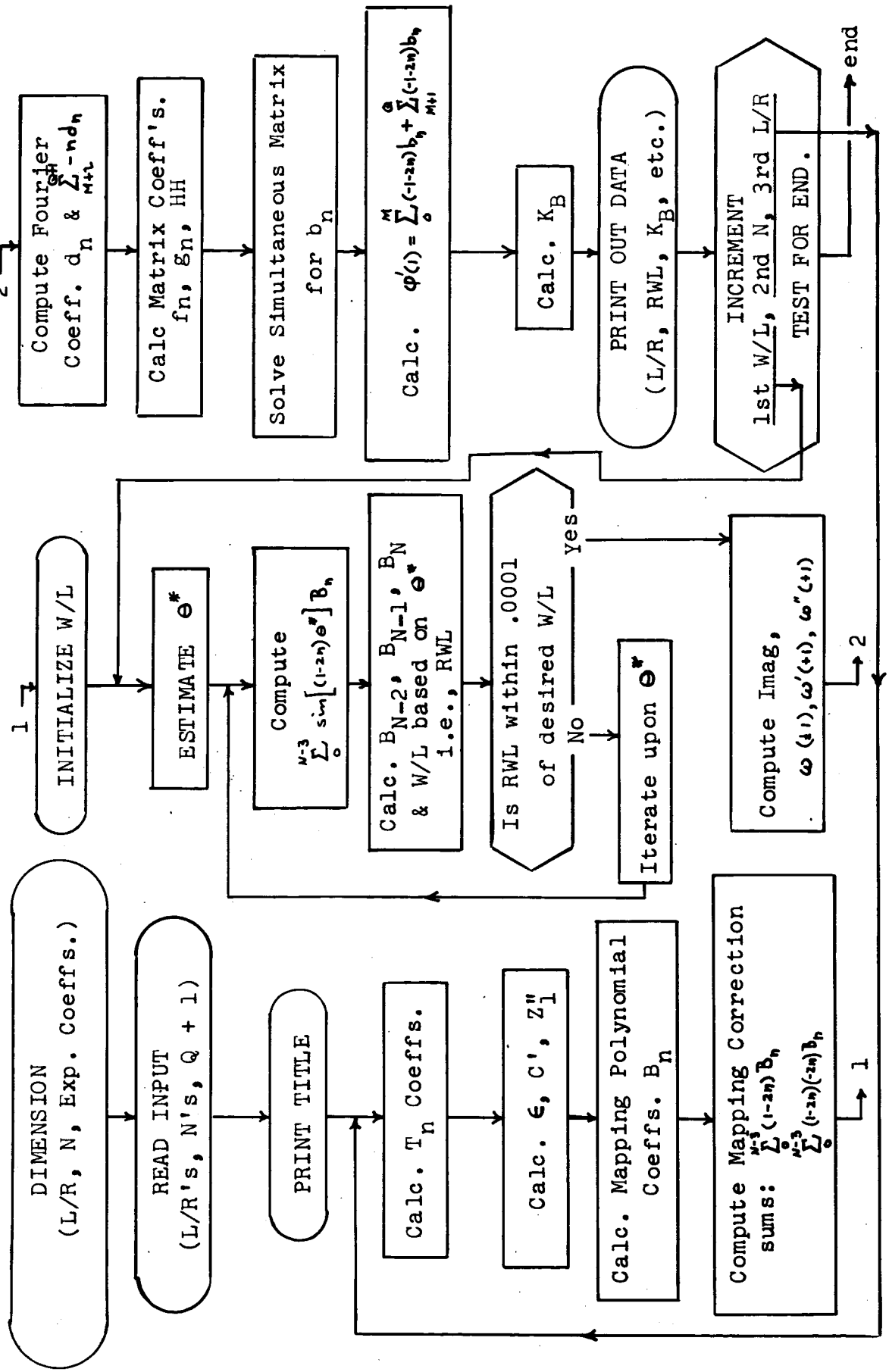

```
#     SEQ  LABL TYP   STATEMENT                                  C ZERO   NOT 0   PLUS   MINUS   ELSE
001.  000000       BNYS  LU225 D2.520 REVISED DEC 20 1966
   .                      SIN
   .                      COS
002.               D   CL(10),NBAR(5)
003.               D   T(25),A(25),EP(30)
004.               D   CCN(12),V(3)
005.               D   EE(30),FF(30),GG(30)
006.               D   DD(30),BB(30)
007.               D   MF(650)
008.               CRDMCL,MNBAR
009.               CRDMF
010.               CRDWL,FWL,CWL
011.                  I=1
012.          R1   CRDCL(I)
013.                  (I=I+1) -MCL                              (R1      (R1
014.                  I=1
015.          R2   CRDNBAR(I)
016.                  (I=I+1) -MNBAR                            (R2      (R2
017.               PL                                  TWIN PLASTC
   .                  IC CRACK TIP STRESS INTENSITY FACTORS
018.               PL
019.               PL
020.               PL BOUNDARY CONDITIONS MATCHED  **  ZPRIME(I+1)=0C
   .                  .0  **  Z2PRIME(I+1)=ACTUAL VALUE  **  IMAGINAC
   .                  RY PART MAP,FN, (THETA) =0.0
021.               PL
022.               PL
023.               PL
024.               PL
025.               PL
026.                  MFOURS=2*MF -1
027.          1       MM=1
028.          2       JJ=1
029.          3       NN=NBAR(JJ) -4
030.                  G1=NN+1
031.                  G2=G1+1
032.                  G3=G2+1
033.                  G4=G3+1
034.                  ADD=MF-G3
035.                  Q1=1.0
036.                  Q=1.0
037.                  S=1.0
038.                  P=0.5
039.                  H=-1.0
040.                  I=1
041.          8       Q=Q1*Q
042.                  (S-1.0)                                   (10      (10
043.                  P=P*S/2.0
044.          10      T(I)=H*P/Q
045.                  Q1=Q1+1.0
046.                  S=S-2.0
047.                  H=-1.0*H
048.                  (I=I+1) -G1                               (8       (8
049.          21      LAMBDA=CL(MM)+1.0
050.                  LMDS=LAMBDA*LAMBDA
```

#	SEQ	LABL	TYP	STATEMENT	C ZERO	NOT 0	PLUS	MINUS	ELSE
051.				QUAN=(LMDS-1.0)/(LMDS+1.0)	[ ]	[ ]	[ ]	[ ]	[ ]
052.				E=2.0*QUAN*QUAN -1.0	[ ]	[ ]	[ ]	[ ]	[ ]
053.				COEF=SQRT.(2.0/(1.0-E))	[ ]	[ ]	[ ]	[ ]	[ ]
054.				ACT1=2.0*SQRT.(2.0)+(3.0+E)/SQRT.(1.0+E)	[ ]	[ ]	[ ]	[ ]	[ ]
055.				ACT2=3.0+E+2.0*SQRT.(2.0+2.0*E)	[ ]	[ ]	[ ]	[ ]	[ ]
056.				AZ2=ACT1/SQRT.(ACT2)	[ ]	[ ]	[ ]	[ ]	[ ]
057.				AZD1=COEF*AZ2	[ ]	[ ]	[ ]	[ ]	[ ]
058.				(E-0.000001)	[ ]	[ ]	[23]	[ ]	[ ]
059.				(E+0.000001)	[ ]	[ ]	[ ]	[23]	[ ]
060.				X=1.5707963268	[ ]	[ ]	[ ]	[ ]	[24]
061.		23		W1=SQRT.(1-E**2)	[ ]	[ ]	[ ]	[ ]	[ ]
062.				W2=-W1/E	[ ]	[ ]	[ ]	[ ]	[ ]
063.				X=ATAN.(W2)	[ ]	[ ]	[ ]	[ ]	[ ]
064.				(E)	[ ]	[ ]	[ ]	[24]	[ ]
065.				X=X+3.1415926536	[ ]	[ ]	[ ]	[ ]	[ ]
066.		24		J=1	[ ]	[ ]	[ ]	[ ]	[ ]
067.		25		W=J	[ ]	[ ]	[ ]	[ ]	[ ]
068.				Y=W*X	[ ]	[ ]	[ ]	[ ]	[ ]
069.				C=2.0*T(J)*COS.(Y)	[ ]	[ ]	[ ]	[ ]	[ ]
070.				U=(-1.0)**W	[ ]	[ ]	[40]	[ ]	[ ]
071.				I=1	[ ]	[ ]	[ ]	[ ]	[ ]
072.				L=J-1	[ ]	[ ]	[ ]	[ ]	[ ]
073.				D=0.0	[ ]	[ ]	[ ]	[ ]	[ ]
074.				K=1	[ ]	[ ]	[ ]	[ ]	[ ]
075.		30		(L-K)	[35]	[ ]	[ ]	[35]	[ ]
076.				Z=L-I	[ ]	[ ]	[ ]	[ ]	[ ]
077.				G=D+2.0*(T(I)*T(L))*COS.(Z*X)	[ ]	[ ]	[ ]	[ ]	[ ]
078.				I=I+1	[ ]	[ ]	[ ]	[ ]	[ ]
079.				L=L-1	[ ]	[ ]	[ ]	[ ]	[ ]
080.				D=G	[ ]	[ ]	[ ]	[ ]	[ ]
081.				K=K+2	[ ]	[ ]	[ ]	[ ]	[ ]
082.				(K-NN-1)	[ ]	[ ]	[ ]	[30]	[ ]
083.		35		B=0.0	[ ]	[ ]	[ ]	[ ]	[50]
084.		40		N=J/2	[ ]	[ ]	[ ]	[ ]	[ ]
085.				B=T(N)*T(N)	[ ]	[ ]	[ ]	[ ]	[ ]
086.				I=1	[ ]	[ ]	[ ]	[ ]	[ ]
087.				L=J-1	[ ]	[ ]	[ ]	[ ]	[ ]
088.				D=0.0	[ ]	[ ]	[ ]	[ ]	[ ]
089.				K=2	[ ]	[ ]	[ ]	[ ]	[ ]
090.		42		(L-K)	[50]	[ ]	[ ]	[50]	[ ]
091.				Z=L-I	[ ]	[ ]	[ ]	[ ]	[ ]
092.				G=D+2.0*(T(I)*T(L))*COS.(Z*X)	[ ]	[ ]	[ ]	[ ]	[ ]
093.				I=I+1	[ ]	[ ]	[ ]	[ ]	[ ]
094.				L=L-1	[ ]	[ ]	[ ]	[ ]	[ ]
095.				D=G	[ ]	[ ]	[ ]	[ ]	[ ]
096.				K=K+2	[ ]	[ ]	[ ]	[ ]	[ ]
097.				(K-NN)	[42]	[ ]	[ ]	[42]	[ ]
098.		50		A(J)=B+C+D	[ ]	[ ]	[ ]	[ ]	[ ]
099.				(J-J+1) -G1	[25]	[ ]	[ ]	[25]	[ ]
100.				EF(1)=(A(1)+2.0+E)/2.0	[ ]	[ ]	[ ]	[ ]	[ ]
101.				EF(2)=(A(1)+A(2)+1.0)/2.0	[ ]	[ ]	[ ]	[ ]	[ ]
102.				I=3	[ ]	[ ]	[ ]	[ ]	[ ]
103.		51		K=I-1	[ ]	[ ]	[ ]	[ ]	[ ]
104.				EF(I)=(A(I)+A(K))/2.0	[ ]	[ ]	[ ]	[ ]	[ ]
105.				(I=I+1) -G1	[51]	[ ]	[ ]	[51]	[ ]
106.				EF(0)=1.0	[ ]	[ ]	[ ]	[ ]	[ ]

#	SEC	LABL	TYP	STATEMENT	C ZERO	NOT 0	PLUS	MINUS	ELSE
107.				EP(1)=EP(1)/2.0	[ ]	[ ]	[ ]	[ ]	[ ]
108.				I=2	[ ]	[ ]	[ ]	[ ]	[ ]
109.		TW1		EPSUM=0.0	[ ]	[ ]	[ ]	[ ]	[ ]
110.				J=1	[ ]	[ ]	[ ]	[ ]	[ ]
111.				K=I-1	[ ]	[ ]	[ ]	[ ]	[ ]
112.		TW2		EPSUM=EPSUM+EP(J)*EP(K)	[ ]	[ ]	[ ]	[ ]	[ ]
113.				J=J+1	[ ]	[ ]	[ ]	[ ]	[ ]
114.				(K=K-1)	[ ]	[ ]	(TW2)	[ ]	[ ]
115.				EP(I)=(EP(I)+EPSUM)/2.0	[ ]	[ ]	[ ]	[ ]	[ ]
116.				(I=I+1) -G1	(TW1)	[ ]	[ ]	(TW1)	[ ]
117.				R=0.0	[ ]	[ ]	[ ]	[ ]	[ ]
118.				I=0	[ ]	[ ]	[ ]	[ ]	[ ]
119.		52		R=R+(1-2*I)*EP(I)	[ ]	[ ]	[ ]	[ ]	[ ]
120.				(I=I+1) -G1	(52)	[ ]	[ ]	(52)	[ ]
121.				RR=0.0	[ ]	[ ]	[ ]	[ ]	[ ]
122.				I=1	[ ]	[ ]	[ ]	[ ]	[ ]
123.		53		RR=RR+2*I*(2*I-1)*EP(I)	[ ]	[ ]	[ ]	[ ]	[ ]
124.				(I=I+1) -G1	(53)	[ ]	[ ]	(53)	[ ]
125.				WL=IWL	[ ]	[ ]	[ ]	[ ]	[ ]
126.		57		TLNH=1.0 + (1.0-WL)*CL(MM)	[ ]	[ ]	[ ]	[ ]	[ ]
127.				LCIF=2.0	[ ]	[ ]	[ ]	[ ]	[ ]
128.				I=1	[ ]	[ ]	[ ]	[ ]	[ ]
129.				J=1	[ ]	[ ]	[ ]	[ ]	[ ]
130.				L=1	[ ]	[ ]	[ ]	[ ]	[ ]
131.				N=1	[ ]	[ ]	[ ]	[ ]	[ ]
132.				O=0.1	[ ]	[ ]	[ ]	[ ]	[ ]
133.		LNH0		LNH=COS.(O)	[ ]	[ ]	[ ]	[ ]	[ ]
134.				K=1	[ ]	[ ]	[ ]	[ ]	[ ]
135.		LNH1		LNH=LNH+EP(K)*COS.((2*K-1)*O)	[ ]	[ ]	[ ]	[ ]	[ ]
136.				(K=K+1) -G1	(LNH1)	[ ]	[ ]	(LNH1)	[ ]
137.				LNH=LNH*COFF	[ ]	[ ]	[ ]	[ ]	[ ]
138.				(TLNH-LNH-0.001)	(LNH6)	[ ]	(LNH2)	[ ]	[ ]
139.				(TLNH-LNH+0.001)	(LNH6)	[ ]	(LNH6)	(LNH4)	[ ]
140.		LNH2		(I-1)	[ ]	[ ]	(LNH3)	[ ]	[ ]
141.				OM=O	[ ]	[ ]	[ ]	[ ]	[ ]
142.				O=O -0.1	[ ]	[ ]	[ ]	[ ]	[ ]
143.				J=2	[ ]	[ ]	[ ]	[ ]	(LNH0)
144.		LNH3		OM=O	[ ]	[ ]	[ ]	[ ]	[ ]
145.				O=(OM+OL)/2	[ ]	[ ]	[ ]	[ ]	[ ]
146.				J=2	[ ]	[ ]	[ ]	[ ]	(LNH0)
147.		LNH4		(J-1)	[ ]	[ ]	(LNH5)	[ ]	[ ]
148.				OL=O	[ ]	[ ]	[ ]	[ ]	[ ]
149.				O=O+0.1	[ ]	[ ]	[ ]	[ ]	[ ]
150.				I=2	[ ]	[ ]	[ ]	[ ]	(LNH0)
151.		LNH5		OL=O	[ ]	[ ]	[ ]	[ ]	[ ]
152.				O=(OM+OL)/2	[ ]	[ ]	[ ]	[ ]	[ ]
153.				I=2	[ ]	[ ]	[ ]	[ ]	(LNH0)
154.		LNH6		O=O	[ ]	[ ]	[ ]	[ ]	[ ]
155.				(L-1)	[ ]	(OMOL)	[ ]	[ ]	[ ]
156.				(N-1)	(CONT)	[ ]	[ ]	[ ]	[ ]
157.		OMOL		(OM-OL-0.00000001)	(WL2)	[ ]	(CONT)	[ ]	[ ]
158.				(OM-OL+0.00000001)	(WL2)	[ ]	(WL2)	(CONT)	[ ]
159.		CONT			[ ]	[ ]	[ ]	[ ]	[ ]
160.				RRR=SIN.(O)	[ ]	[ ]	[ ]	[ ]	[ ]
161.				K=1	[ ]	[ ]	[ ]	[ ]	[ ]
162.		RRR1		RRR=RRR -EP(K)*SIN.((2*K-1)*O)	[ ]	[ ]	[ ]	[ ]	[ ]

#	SEQ	LABL	TYP	STATEMENT	C ZERO	NOT 0	PLUS	MINUS	ELSE
163.				[K=K+1] -G1	[RRR1]	[ ]	[ ]	[RRR1]	[ ]
164.				CCN[1]=2*G2 -1	[ ]	[ ]	[ ]	[ ]	[ ]
165.				CCN[2]=2*G3 -1	[ ]	[ ]	[ ]	[ ]	[ ]
166.				CCN[3]=2*G4 -1	[ ]	[ ]	[ ]	[ ]	[ ]
167.				CCN[4]=R	[ ]	[ ]	[ ]	[ ]	[ ]
168.				CCN[5]=2*G2*CON[1]	[ ]	[ ]	[ ]	[ ]	[ ]
169.				CCN[6]=2*G3*CON[2]	[ ]	[ ]	[ ]	[ ]	[ ]
170.				CCN[7]=2*G4*CON[3]	[ ]	[ ]	[ ]	[ ]	[ ]
171.				CCN[8]=AZZ-RR	[ ]	[ ]	[ ]	[ ]	[ ]
172.				CCN[9]=SIN.[CON[1]*0]	[ ]	[ ]	[ ]	[ ]	[ ]
173.				CCN[10]=SIN.[CCN[2]*0]	[ ]	[ ]	[ ]	[ ]	[ ]
174.				CCN[11]=SIN.[CCN[3]*0]	[ ]	[ ]	[ ]	[ ]	[ ]
175.				CCN[12]=RRR	[ ]	[ ]	[ ]	[ ]	[ ]
176.				SMFCS,[3,%CON%,%V%]	[ ]	[ ]	[ ]	[ ]	[ ]
177.				EP[G2]=V[1]	[ ]	[ ]	[ ]	[ ]	[ ]
178.				EP[G3]=V[2]	[ ]	[ ]	[ ]	[ ]	[ ]
179.				EP[G4]=V[3]	[ ]	[ ]	[ ]	[ ]	[ ]
180.		CR1		CCR=COS.[0]	[ ]	[ ]	[ ]	[ ]	[ ]
181.				K=1	[ ]	[ ]	[ ]	[ ]	[ ]
182.		CR2		CCR=COR+EP[K]*CCS.[[2*K-1]*0]	[ ]	[ ]	[ ]	[ ]	[ ]
183.				[K=K+1] -G4	[CR2]	[ ]	[ ]	[CR2]	[ ]
184.				CCR=COR*COEF	[ ]	[ ]	[ ]	[ ]	[ ]
185.				RWL=[LAMBDA-COR]/CL[MM]	[ ]	[ ]	[ ]	[ ]	[ ]
186.				DIF=ABS.[WL-RWL]	[ ]	[ ]	[ ]	[ ]	[ ]
187.				[LDIF-DIF]	[ ]	[ ]	[ ]	[WL1]	[ ]
188.				LDIF=DIF	[ ]	[ ]	[ ]	[ ]	[ ]
189.				LRWL=RWL	[ ]	[ ]	[ ]	[ ]	[ ]
190.				LC=0	[ ]	[ ]	[ ]	[ ]	[ ]
191.				LCOR=COR	[ ]	[ ]	[ ]	[ ]	[ ]
192.				VV1=V[1]	[ ]	[ ]	[ ]	[ ]	[ ]
193.				VV2=V[2]	[ ]	[ ]	[ ]	[ ]	[ ]
194.				VV3=V[3]	[ ]	[ ]	[ ]	[ ]	[ ]
195.		WL1		[RWL]	[ ]	[ ]	[ ]	[WL2]	[ ]
196.				[RWL-3]	[ ]	[ ]	[WL2]	[ ]	[ ]
197.				[WL-RWL-0.0001]	[64]	[ ]	[62]	[ ]	[ ]
198.				[WL-RWL+0.0001]	[64]	[ ]	[64]	[63]	[ ]
199.		62		[L-1]	[ ]	[ ]	[UP]	[ ]	[ ]
200.				OL=O	[ ]	[ ]	[ ]	[ ]	[ ]
201.				O=O+0.01	[ ]	[ ]	[ ]	[ ]	[ ]
202.				N=2	[ ]	[ ]	[ ]	[ ]	[LNH6]
203.		UP		OL=O	[ ]	[ ]	[ ]	[ ]	[ ]
204.				O=[OM+OL]/2	[ ]	[ ]	[ ]	[ ]	[ ]
205.				N=2	[ ]	[ ]	[ ]	[ ]	[LNH6]
206.		63		[N-1]	[ ]	[ ]	[DOWN]	[ ]	[ ]
207.				OM=O	[ ]	[ ]	[ ]	[ ]	[ ]
208.				O=O-0.01	[ ]	[ ]	[ ]	[ ]	[ ]
209.				L=2	[ ]	[ ]	[ ]	[ ]	[LNH6]
210.		DOWN		OM=O	[ ]	[ ]	[ ]	[ ]	[ ]
211.				O=[OM+OL]/2	[ ]	[ ]	[ ]	[ ]	[ ]
212.				L=2	[ ]	[ ]	[ ]	[ ]	[LNH6]
213.		WL2		[N-1]	[ ]	[WL3]	[ ]	[ ]	[ ]
214.				[L-1]	[ ]	[WL3]	[ ]	[ ]	[ ]
215.				[WL-IWL]	[ ]	[90]	[ ]	[ ]	[ ]
216.			PL	CRACK LENGTH F MAP TERMS	[ ]	[ ]	[ ]	[ ]	[ ]
217.			PV	CL[MM],E,G4	[ ]	[ ]	[ ]	[ ]	[ ]
218.			PL		[ ]	[ ]	[ ]	[ ]	[ ]

```
#     SEQ  LABL TYP  STATEMENT                                  C ZERO    NOT 0     PLUS      MINUS     ELSE
219.            PL                                              (    )    (    )    (    )    (    )    (90  )
220.       WL3      RWL=LRWL                                    (    )    (    )    (    )    (    )    (    )
221.                0=L0                                        (    )    (    )    (    )    (    )    (    )
222.                CCR=LCOR                                    (    )    (    )    (    )    (    )    (    )
223.                EP(G2)=VV1                                  (    )    (    )    (    )    (    )    (    )
224.                EP(G3)=VV2                                  (    )    (    )    (    )    (    )    (    )
225.                EP(G4)=VV3                                  (    )    (    )    (    )    (    )    (    )
226.       64       0=0                                         (    )    (    )    (    )    (    )    (    )
227.                RFE=LAMBDA*COR                              (    )    (    )    (    )    (    )    (    )
228.       IM1      IMAG=SIN.(C)                                (    )    (    )    (    )    (    )    (    )
229.                J=1                                         (    )    (    )    (    )    (    )    (    )
230.       IM2      IMAG=IMAG+EP(J)*SIN.( (2*J-1)*0 )           (    )    (    )    (    )    (    )    (    )
231.                (J=J+1) -G4                                 (IM2 )    (    )    (    )    (IM2 )    (    )
232.                ZP1=0.0                                     (    )    (    )    (    )    (    )    (    )
233.                ZM1=0.0                                     (    )    (    )    (    )    (    )    (    )
234.                J=0                                         (    )    (    )    (    )    (    )    (    )
235.       70       ZP1=ZP1+EP(J)                               (    )    (    )    (    )    (    )    (    )
236.                ZM1=ZM1-EP(J)                               (    )    (    )    (    )    (    )    (    )
237.                (J=J+1) -G4                                 (70  )    (    )    (    )    (70  )    (    )
238.                ZP1=COEF*ZP1                                (    )    (    )    (    )    (    )    (    )
239.                ZM1=COEF*ZM1                                (    )    (    )    (    )    (    )    (    )
240.                J=0                                         (    )    (    )    (    )    (    )    (    )
241.                ZPRIME1=0.0                                 (    )    (    )    (    )    (    )    (    )
242.       72       ZPRIME1=ZPRIME1+(1+2*J)*EP(J)               (    )    (    )    (    )    (    )    (    )
243.                (J=J+1) -G4                                 (72  )    (    )    (    )    (72  )    (    )
244.                ZPRIME1=COEF*ZPRIME1                        (    )    (    )    (    )    (    )    (    )
245.                J=1                                         (    )    (    )    (    )    (    )    (    )
246.                Z2PRIME1=0.0                                (    )    (    )    (    )    (    )    (    )
247.       74       Z2PRIME1=Z2PRIME1 +2*J*(2*J-1)*EP(J)        (    )    (    )    (    )    (    )    (    )
248.                (J=J+1) -G4                                 (74  )    (    )    (    )    (74  )    (    )
249.                Z2PRIME1=COEF*Z2PRIME1                      (    )    (    )    (    )    (    )    (    )
250.                PIP=0.0                                     (    )    (    )    (    )    (    )    (    )
251.                N=-1                                        (    )    (    )    (    )    (    )    (    )
252.                L=1                                         (    )    (    )    (    )    (    )    (    )
253.       D1       K=0                                         (    )    (    )    (    )    (    )    (    )
254.                SN=0.0                                      (    )    (    )    (    )    (    )    (    )
255.       D2       LL=1-2*K-N                                  (    )    (    )    (D4  )    (D3  )    (    )
256.                SN=SN+EP(K)*0                               (    )    (    )    (    )    (    )    (D5  )
257.       D3       SN=SN+EP(K)*SIN.(*LL*0)/LL                  (    )    (    )    (    )    (    )    (D5  )
258.       D4       SN=SN+EP(K)*SIN.(LL*0)/LL                   (    )    (    )    (    )    (    )    (    )
259.       D5       (K=K+1) -G4                                 (D2  )    (    )    (    )    (D2  )    (    )
260.                (N+2*G2+1)                                  (    )    (    )    (    )    (D6  )    (    )
261.                DD(L)=COEF*SN*CCR*SIN.(-N*0)/N              (    )    (    )    (    )    (    )    (    )
262.                DD(L)=DD(L)/3.14159265                      (    )    (    )    (    )    (    )    (    )
263.                L=L+1                                       (    )    (    )    (    )    (    )    (    )
264.                (N=N-2)                                     (    )    (    )    (    )    (    )    (D1  )
265.       D6       NF=N/3.14159265                             (    )    (    )    (    )    (    )    (    )
266.                PIP=PIP+NF*(COEF*SN*COR*SIN.(-N*0)/N)       (    )    (    )    (    )    (    )    (    )
267.                (N=N-2) +MFOURS                             (D1  )    (    )    (D1  )    (    )    (    )
268.       EEX0     NSTAR=NBAR(JJ)-2                            (    )    (    )    (    )    (    )    (    )
269.                N=0                                         (    )    (    )    (    )    (    )    (    )
270.       EEX1     EE(N)=(1-2*N)*EP(N)                         (    )    (    )    (    )    (    )    (    )
271.                (N=N+1) -NSTAR                              (EEX1)    (    )    (    )    (EEX1)    (    )
272.                FF(0)=1                                     (    )    (    )    (    )    (    )    (    )
273.                N=1                                         (    )    (    )    (    )    (    )    (    )
274.       FFX1     FF(N)=0.0                                   (    )    (    )    (    )    (    )    (    )
```

```
#      SEQ  LABL TYP                STATEMENT                    C ZERO    NOT 0     PLUS      MINUS     ELSE
275.                              (N=N+1) -NSTAR                 (FFX1)    (   )     (   )     (FFX1)    (   )
276.                              N1=0                           (   )     (   )     (   )     (   )     (   )
277.              FFX2            FF(N1)=FF(N1)/EE(0)            (   )     (   )     (   )     (   )     (   )
278.                              N2=N1+1                        (   )     (   )     (   )     (   )     (   )
279.                              N=1                            (   )     (   )     (   )     (   )     (   )
280.              FFX3            FF(N2)=FF(N2)-FF(N1)*EE(N)     (   )     (   )     (   )     (   )     (   )
281.                              N=N+1                          (   )     (   )     (   )     (   )     (   )
282.                              (N2=N2+1) -NSTAR               (FFX3)    (   )     (   )     (FFX3)    (   )
283.                              (N1=N1+1) -NSTAR               (FFX2)    (   )     (   )     (FFX2)    (   )
284.                              N=0                            (   )     (   )     (   )     (   )     (   )
285.              GGX1            GG(N)=0.0                      (   )     (   )     (   )     (   )     (   )
286.                              (N=N+1) -NSTAR                 (GGX1)    (   )     (   )     (GGX1)    (   )
287.                              N=0                            (   )     (   )     (   )     (   )     (   )
288.              GGX2            I=0                            (   )     (   )     (   )     (   )     (   )
289.              GGX3            N1=N+I+2                       (   )     (   )     (   )     (   )     (   )
290.                              GG(N)=GG(N)+FF(I)*EP(N1)       (   )     (   )     (   )     (   )     (   )
291.                              (I=I+1) +N-NSTAR               (GGX3)    (   )     (   )     (GGX3)    (   )
292.                              (N=N+1) -NSTAR                 (GGX2)    (   )     (   )     (GGX2)    (   )
293.                              N1=NSTAR+1                     (   )     (   )     (   )     (   )     (   )
294.                              N2=N1+(N1+1)                   (   )     (   )     (   )     (   )     (   )
295.                              I=1                            (   )     (   )     (   )     (   )     (   )
296.              HHX1            HH(I)=0.0                      (   )     (   )     (   )     (   )     (   )
297.                              (I=I+1) -N2                    (HHX1)    (   )     (   )     (HHX1)    (   )
298.                              P=1                            (   )     (   )     (   )     (   )     (   )
299.              HHX2            J=0                            (   )     (   )     (   )     (   )     (   )
300.                              K=P-1                          (   )     (   )     (   )     (   )     (   )
301.                              I=1+K*(NSTAR+2)                (   )     (   )     (   )     (   )     (   )
302.              HHX3            HH(I)=(1-J)*GG(K)              (   )     (   )     (   )     (   )     (   )
303.                              I=I+1                          (   )     (   )     (   )     (   )     (   )
304.                              J=J+2                          (   )     (   )     (   )     (   )     (   )
305.                              (K=K+1) -NSTAR                 (HHX3)    (   )     (   )     (HHX3)    (   )
306.                              I=P+(P-1)*(NSTAR+2)            (   )     (   )     (   )     (   )     (   )
307.                              HH(I)=HH(I)+1                  (   )     (   )     (   )     (   )     (   )
308.                              I=P+(NSTAR+2)                  (   )     (   )     (   )     (   )     (   )
309.                              HH(I)=DD(P)                    (   )     (   )     (   )     (   )     (   )
310.                              (P=P+1) -N1                    (HHX2)    (   )     (   )     (HHX2)    (   )
311.                              SPECS.(N1,*HH*,*BB*)           (   )     (   )     (   )     (   )     (   )
312.                              PHIPRIME1=0.0                  (   )     (   )     (   )     (   )     (   )
313.                              K=1                            (   )     (   )     (   )     (   )     (   )
314.              80              PHIPRIME1=PHIPRIME1+(1-2*K)*BB(K)  (   )  (   )     (   )     (   )     (   )
315.                              (K=K+1) -N1                    (80       (   )     (   )     (80       (   )
316.                              PHIPRIME1=2*PHIPRIME1          (   )     (   )     (   )     (   )     (   )
317.                              PIP=2*PIP                      (   )     (   )     (   )     (   )     (   )
318.                              PHIPRIME1=PHIPRIME1 +PIP       (   )     (   )     (   )     (   )     (   )
319.                              KTP=2.0*SQRT.(1.0/A2D1)*PHIPRIME1  (   )  (   )     (   )     (   )     (   )
320.                              (WL-IWL)                       (   )     (PRT1)    (   )     (   )     (   )
321.                    PL   CRACK LENGTH        F          MAP TERMS  (   )  (   )     (   )     (   )     (   )
322.                    PV CL(MM),E,G4                        (   )     (   )     (   )     (   )     (   )
323.                    PL                                    (   )     (   )     (   )     (   )     (   )
324.                    PL                                    (   )     (   )     (   )     (   )     (   )
325.              PRT1  PL     RATIO W/L    PLASTIC LENGTH     Z(+1)     C
                                Z(-1)          ZPRIME(+1)     Z2PRIME(1)  C
                              ACT.Z2PR(1)       IMAG          (   )     (   )     (   )     (   )     (   )
326.                    PV RWL,RPF,ZP1,ZM1,ZPRIME1,Z2PRIME1,A2D1,IMAG  (   )  (   )  (   )  (   )  (   )
327.                    PL       THETA        FOUR.TERMS     ADDED PHIPR.  C
                                PHIPRIME1      K(PLASTIC)     (   )     (   )     (   )     (   )     (   )
```

#	SEQ	LABL	TYP	STATEMENT	C ZERO	NOT 0	PLUS	MINUS	ELSE
328.			FV	O,ADD,PIP,PHIPRIME1,KTP	[ ]	[ ]	[ ]	[ ]	[ ]
329.			PL		[ ]	[ ]	[ ]	[ ]	[ ]
330.			PL		[ ]	[ ]	[ ]	[ ]	[ ]
331.		90		[WL-0.05]	[ ]	[91]	[ ]	[ ]	[ ]
332.				WL=CWL	[ ]	[ ]	[ ]	[ ]	[57]
333.		91		[WL=WL+CWL] -FWL	[57]	[ ]	[ ]	[57]	[ ]
334.				[J=JJ+1] -MNBAR	[ ]	[ ]	[96]	[ ]	[ ]
335.			SL		[ ]	[ ]	[ ]	[ ]	[3]
336.		96		[MM=MM+1] -MCL	[ ]	[ ]	[TOM]	[ ]	[ ]
337.				SWT.[100]	[ ]	[ ]	[ ]	[ ]	[ ]
338.			SL		[ ]	[ ]	[ ]	[ ]	[2]
339.		TOM	END	OF PROGRAM	[ ]	[ ]	[ ]	[ ]	[ ]

*****SYMBOL TABLE*****

A	ADD	ACT1
ACT2	AZ2	A2D1
BB	*ATAN	B
*ABS	COS	CL
CON	CWL	COEF
C	DD	D
CONT	*CR1	COR
CR2	EP	EE
E	EPSUM	DIF
DOWN	FF	FWL
D1	D2	D4
D3	GG	G1
G2	G3	G4
G	HH	H
D5	D6	*EEXO
EEX1	IWL	I
*IM1	IMAG	IM2
FFX1	FFX2	FFX3
GGX1	GGX2	GGX3
HHX1	HHX2	HHX3
JJ	J	K
KTP	LAMBDA	LMDS
L	LDIF	LNHO
LNH	MCL	MNBAR
MF	MFOURS	MM
LNH1	NBAR	NN
N	LNH6	LNH2
LNH4	O	LNH3
OM	OL	LNH5
OMOL	P	LRWL
LO	LCOR	PIP
LL	Q1	Q
QUAN	NP	NSTAR

N1
R2
RRR
RPE
PRT1
SQRT
*SWT
TW2
*U
VV1
W1
WL
X
Z
ZPRIME1
*RUNEND
R
RRR1
N2
SIN
SMEQS
T
TLNH
UP
VV2
W2
WL2
WL3
ZP1
Z2PRIME1
R1
RR
RWL
PHIPRIME1
S
SN
TW1
TOM
V
VV3
W
WL1
Y
ZM1

UNUSED MEMORY FROM (OCTAL) 11454 TO (OCTAL) 12640.

TWIN PLASTIC CRACK TIP STRESS INTENSITY FACTORS

BOUNDARY CONDITIONS MATCHED ** ZPRIME[+1]=0.0 ** Z2PRIME[+1]=ACTUAL VALUE ** IMAGINARY PART MAP.FN. [THETA] =0.0

CRACK LENGTH	E	MAP TERMS					
2.0000000+00	2.8000000-01	2.6000000+01					
RATIO W/L	PLASTIC LENGTH	Z[+1]	Z[-1]	ZPRIME[+1]	Z2PRIME[1]	ACT,Z2PR[1]	IMAG
4.9966261-02	9.9932522-02	2.9999995+00	-2.9999996+00	9.7012768-11	3.7500000+00	3.7500000+00	-4.5474735-12
THETA	FOUR.TERMS	ADDED PHIPR.	PHIPRIME1	K[PLASTIC]			
2.3093750-01	7.5000000+01	2.5111949-02	-2.7125790-01	-2.8015395-01			
RATIO W/L	PLASTIC LENGTH	Z[+1]	Z[-1]	ZPRIME[+1]	Z2PRIME[1]	ACT,Z2PR[1]	IMAG
1.0001374-01	2.0002747-01	3.0000021+00	-3.0000022+00	9.7012768-11	3.7500000+00	3.7500000+00	3.6379788-12
THETA	FOUR.TERMS	ADDED PHIPR.	PHIPRIME1	K[PLASTIC]			
3.2687500-01	7.5000000+01	1.6647337-02	-3.8801951-01	-4.0074482-01			
RATIO W/L	PLASTIC LENGTH	Z[+1]	Z[-1]	ZPRIME[+1]	Z2PRIME[1]	ACT,Z2PR[1]	IMAG
2.0001426-01	4.0002852-01	3.0000011+00	-3.0000011+00	-1.4551915-10	3.7500000+00	3.7500000+00	6.3664629-12
THETA	FOUR.TERMS	ADDED PHIPR.	PHIPRIME1	K[PLASTIC]			
4.6187500-01	7.5000000+01	1.3411697-02	-5.6154360-01	-5.7995974-01			
RATIO W/L	PLASTIC LENGTH	Z[+1]	Z[-1]	ZPRIME[+1]	Z2PRIME[1]	ACT,Z2PR[1]	IMAG
3.0003820-01	6.0007640-01	2.9999948+00	-2.9999949+00	1.9402554-10	3.7500000+00	3.7500000+00	1.1823431-11
THETA	FOUR.TERMS	ADDED PHIPR.	PHIPRIME1	K[PLASTIC]			
5.6359375-01	7.5000000+01	-4.0204782-03	-6.8581196-01	-7.0830355-01			
RATIO W/L	PLASTIC LENGTH	Z[+1]	Z[-1]	ZPRIME[+1]	Z2PRIME[1]	ACT,Z2PR[1]	IMAG
3.9997641-01	7.9995282-01	3.0000046+00	-3.0000047+00	5.7601331-11	3.7500000+00	3.7500000+00	-1.6484591-12
THETA	FOUR.TERMS	ADDED PHIPR.	PHIPRIME1	K[PLASTIC]			
6.4812500-01	7.5000000+01	-4.2080970-02	-7.9658207-01	-8.2270642-01			
RATIO W/L	PLASTIC LENGTH	Z[+1]	Z[-1]	ZPRIME[+1]	Z2PRIME[1]	ACT,Z2PR[1]	IMAG
4.9993298-01	9.9986596-01	2.9999981+00	-2.9999982+00	0.0000000+00	3.7499999+00	3.7500000+00	5.4569682-12
THETA	FOUR.TERMS	ADDED PHIPR.	PHIPRIME1	K[PLASTIC]			
7.2359375-01	7.5000000+01	2.1278493-02	-8.8732436-01	-9.1642466-01			
RATIO W/L	PLASTIC LENGTH	Z[+1]	Z[-1]	ZPRIME[+1]	Z2PRIME[1]	ACT,Z2PR[1]	IMAG
5.9994823-01	1.1998965+00	2.9999972+00	-2.9999973+00	-1.9402554-10	3.7500000+00	3.7500000+00	0.0000000+00
THETA	FOUR.TERMS	ADDED PHIPR.	PHIPRIME1	K[PLASTIC]			
7.8468750-01	7.5000000+01	-4.4018162-02	-9.8014020-01	-1.0122844+00			
RATIO W/L	PLASTIC LENGTH	Z[+1]	Z[-1]	ZPRIME[+1]	Z2PRIME[1]	ACT,Z2PR[1]	IMAG
6.9999469-01	1.3999894+00	2.9999983+00	-2.9999984+00	2.9103830-10	3.7500000+00	3.7500000+00	1.5461410-11
THETA	FOUR.TERMS	ADDED PHIPR.	PHIPRIME1	K[PLASTIC]			
8.4234375-01	7.5000000+01	2.3777460-03	-1.0686110+00	-1.1036567+00			

RATIO W/L	PLASTIC LENGTH	Z[+1]	Z[-1]	ZPRIME[+1]	Z2PRIME[1]	ACT.Z2PR[1]	IMAG
8.0001654-01	1.6000331+00	2.9999615+00	-2.9999616+00	0.0000000+00	3.7499999+00	3.7500000+00	0.0000000+00
THETA	FOUR.TERMS	ADDED PHIPR.	PHIPRIME1	K[PLASTIC]			
8.8523437-01	7.5000000+01	9.2966865-02	-1.1275338+00	-1.1645119+00			

TYPE #END# STATEMENT EXECUTED.
MAY 11 67 07 46.7
AUTHORIZED TIME LEFT IS 019 HR 58.7 MIN

VI. References

1. P. C. Paris, and G. C. Sih, "Stress Analysis of Cracks", authorized reprint from the copyrighted Symposium on Fracture Toughness Testing and its Applications, Special Technical Publication No. 381, American Society for Testing and Materials, (1965).

2. G. R. Irwin, "Plastic Zone Near a Crack and Fracture Toughness", Proceedings of the 7th Sagamore Ordnance Material Research Conference, Report MeTE 661-611/F, Syracuse Research Institute, (Aug. 1960), p. IV-63.

3. D. S. Dugdale, "Yielding of Steel Sheets Containing Slits", Journal of the Mechanics and Physics of Solids, Vol. 8, (1960), pp. 100-104.

4. A. R. Rosenfield, P. K. Dai, and G. T. Hahn, "Crack Extension and Propagation Under Plane Stress" preprint of International Conference on Fracture, Sendai, Japan, (Sept., 1965), No. 1, pp. A-179 to A-226.

5. A. S. Kobayashi, and R. C. Brown, "A Plasticity Correction for a Single-Edge Cracked Specimen in Tension", The Trend in Engineering, Quarterly Journal of the University of Washington - College of Engineering, Vol 19, No. 1, (Jan., 1967) pp. 8-12 and 36.

6. N. I. Muskhelishvili, Some Basic Problems of the Mathematical Theory of Elasticity, P. Noordhoff Ltd., Groningen, Holland, (1953).

7. R. Roberts, and T. Rich, "Stress Intensity Factors for an Infinite Plate with Radial Cracks Emanating from an Internal Hole and Subjected to Cylindrical Bending", A progress report prepared for N.A.S.A. under Contract NGR 39-007-011: Lehigh University, (April, 1966). [Note: Parts of this report have been accepted for publication in the Journal of Applied Mechanics].

8. E. J. Brown, "Thermal Stresses and Elastic-Plastic Stress Distribution in Bonded Dissimilar Media with Cuts along the Interface", Unpublished Ph.D. dissertation, Lehigh University, (1966).

VII Tables

TABLE 1

Table for L/R

x \ y	.05	.1	.2	.3	.4	.5	.6	.7	.8	.9	1.0
0.5	.526	.556	.625	.714	.833	1.00	1.25	1.67	2.50	5.00	∞
1	1.05	1.11	1.25	1.43	1.67	2.00	2.50	3.33	5.00	10.00	↓
2	2.11	2.22	2.50	2.86	3.33	4.00	5.00	6.67	10.00	20.00	
3	3.16	3.33	3.75	4.29	5.00	6.00	7.50	10.00	15.00	30.00	
4	4.21	4.44	5.00	5.71	6.67	8.00	10.00	13.33	20.00	40.00	
5	5.26	5.56	6.25	7.14	8.33	10.00	12.50	16.67	25.00	50.00	
6	6.32	6.67	7.50	8.57	10.00	12.00	15.00	20.00	30.00	60.00	
7	7.37	7.78	8.75	10.00	11.67	14.00	17.50	23.33	35.00	70.00	
8	8.42	8.89	10.00	11.43	13.33	16.00	20.00	26.67	40.00	80.00	
9	9.47	10.00	11.25	12.86	15.00	18.00	22.50	30.00	45.00	90.00	
10	10.53	11.11	12.50	14.29	16.67	20.00	25.00	33.33	50.00	100.00	

TABLE 2

a.) Q = 99, L = 2.0

$-K_B$

y \ M	15	20	22	24	46
.05	.2760	.2778	.2770	.2760	.2770
.30	.6885	.6863	.6841	.6860	.6875
.60			.9646	.9647	

b.) M = 22

$-K_B$

L = 2.0	Q - M	L = 10.0	
y = .192		y = .485	y = .915
.5665	50	1.873	2.438
.5635	75	1.886	2.473
.5617	100	1.898	2.447
.5597	150	1.893	2.455
.5586	200	1.886	2.461
.5578	250	1.896	2.463
.5576	275	1.895	2.453

NOTE: N = M + 4

"Convergence Check for Stress Intensity Factors"

k=1

TABLE 3

L = 10, M = 24, Q = 99

y	$-K_{computer}$	$-K_{approx.\ check}$
.0499	.6316	.6173
.0994	.8849	.8999
.1848	1.1918	1.1919 *
.2002	1.2374	1.2657
.2991	1.4897	1.5267
.4004	1.6956	1.7431
.4852	1.8399	1.8855 *
.5009	1.8644	1.9090
.5997	2.0040	2.0073
.6990	2.1444	2.2248
.7996	2.3133	2.3294
.9010	2.5194	2.4280
.9153	2.552	2.473 *

* M = 22

"Approximate Check Against Internal Straight Crack"

k=1

TABLE 4

$-K_B$

L/R \ y	.05	.1	.2	.3	.4	.5
1	.207					
2	.277	.410	.557	.686	.812	.898
3	.359	.502	.692	.856	.986	1.099
4	.390	.562	.807	.970	1.113	1.240
5	.452	.643	.880	1.094	1.238	1.376
10	.617	.900	1.27	1.53	1.74	1.91

"Plastic Stress Intensity Factors"

k=1

TABLE 5

a.) Q = 99, L = 2.0

$-K_B$

y \ M	13	20	22	23	24
.10	.4020	.4008	.4003	.4015	.4007
.80	1.1882	1.1791	1.1723	1.1884	1.1645

b.) M = 24

$-K_B$

L = 0.5		Q - M	L = 2.0	
y = .10	y = .80		y = .10	y = .80
.2095	.5962	50	.4120	1.1615
.1992	.5900	75	.4007	1.1645
.1958	.5863	100	.4039	1.1667
.2043	.5815	150	.4007	1.1707
.1983	.5782	200	.4027	1.1742
.2027	.5755	250	.4057	1.1771
.1994	.5743	275	.4021	1.1782

"Convergence Check for Stress Intensity Factors"

k=2

TABLE 6

$-K_B$

L/R \ y	.05	.1	.2	.3	.4	.5	.6	.7	.8
.5	.145	.199	.284	.347	.406	.455	.480	.536	.590
1	.201	.291	.408	.487	.570	.646	.690	.767	.816
2	.280	.401	.580	.708	.823	.916	1.012	1.104	1.165
3	.344	.500	.702	.858	1.004	1.133	1.276	1.363	1.440
4	.411	.565	.813	1.003	1.175	1.322	1.459	1.584	1.700
5	.454	.649	.909	1.117	1.317	1.476	1.637	1.782	1.922
10	.643	.912	1.283	1.607	1.870	2.087	2.323	2.532	2.720
15	.796	1.123	1.597	1.950	2.273	2.574	2.836	3.099	3.349
20	.916	1.287	1.837	2.267	2.650	2.963	3.305	3.585	3.880
25	1.021	1.430	2.043	2.545	2.961	3.331	3.681	4.001	4.332
30	1.114	1.561	2.231	2.785	3.233	3.664	4.020	4.395	4.778

"Plastic Stress Intensity Factors"

k=2

TABLE 7

'K_A'

L/R \ k	1	2
.5	1.224	1.296
.6	1.243	1.337
.7	1.263	1.374
.8	1.277	1.408
.9	1.292	1.441
1	1.307	1.472
1.5	1.381	1.620
2	1.458	1.761
3	1.611	2.016
4	1.756	2.246
5	1.892	2.455
6	2.018	2.650
7	2.138	2.831
8	2.251	3.004
9	2.361	3.165
10	2.463	3.317
15		4.001
30		5.568
		TAKEN FROM REF. [7]

"Elastic Stress Intensity Factors"

TABLE 8

σ_∞ / Y

	x \ y	.05	.1	.2	.3	.4	.5	.6	.7	.8
k=1	2	.210	.280	.399	.516	.621	.720			
	3	.222	.319	.447	.562	.672	.758			
	4	.246	.341	.472	.594	.705	.774			
k=2	.5	.121	.158	.239	.306	.366	.428	.514	.595	.695
	.75	.136	.189	.269	.342	.410	.487	.565	.658	.746
	1	.140	.205	.295	.373	.446	.517	.600	.686	.777
	1.5	.152	.219	.324	.404	.489	.567	.643	.717	.809
	2	.162	.223	.337	.425	.512	.587	.669	.737	.822
	3	.173	.246	.352	.444	.535	.610	.689	.762	.836
	4	.182	.258	.369	.460	.551	.624	.697	.768	.844
	5	.184	.262	.385	.472	.562	.625	.702	.777	.846
	6	.185	.263	.390	.484	.564	.628	.707	.783	.855
	7	.189	.264	.393	.485	.566	.639	.712	.783	.
	8	.191	.267	.398	.487	.566	.642	.717	.784	.
	9	.191	.271	.400	.492	.567	.644	.719	.785	.
	10	.192	.272	.400	.492	.568	.651	.719		

cont'd. next page

DUGDALE

x \ σ_∞/Y	y = 0	.1	.2	.3	.4	.5	.6	.7	.8	.9	1.0
∞	0	.0123	.0489	.1090	.1910	.2929	.4122	.5460	.6910	.8434	1.

"Plastic Enclave Sizes"

VIII Figures

FIGURE 1

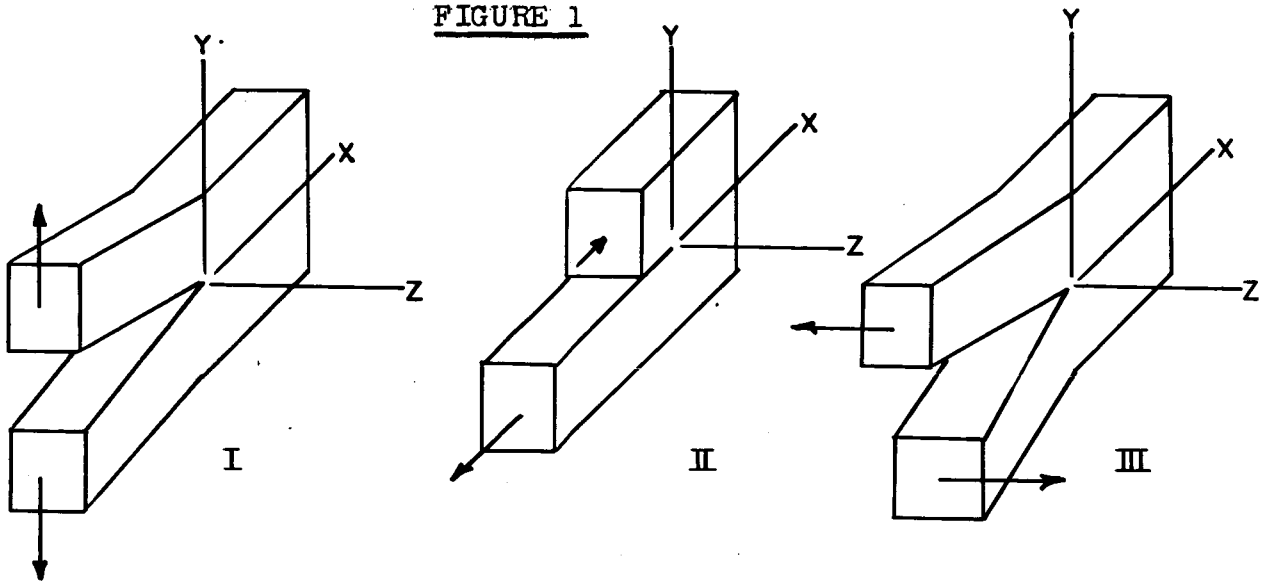

Basic Modes of Crack Surface Displacement

FIGURE 2

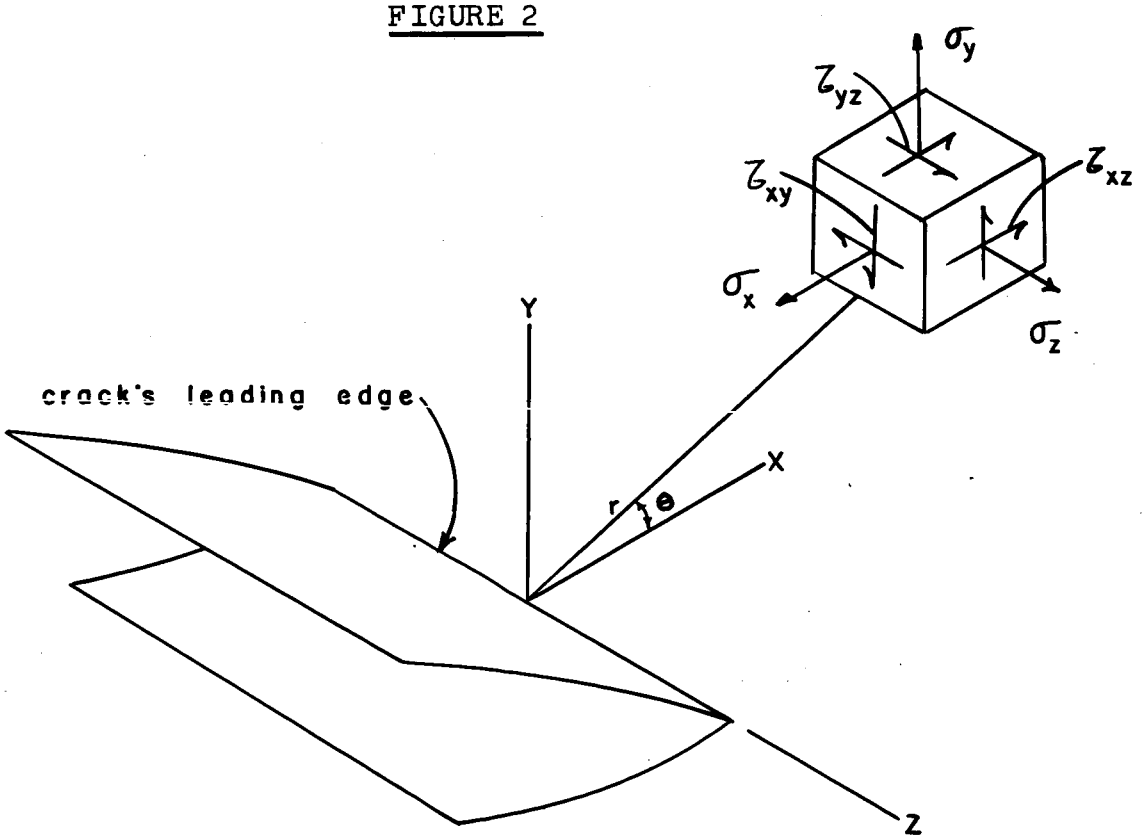

Coordinant Notation and Stress Components

FIGURE 3

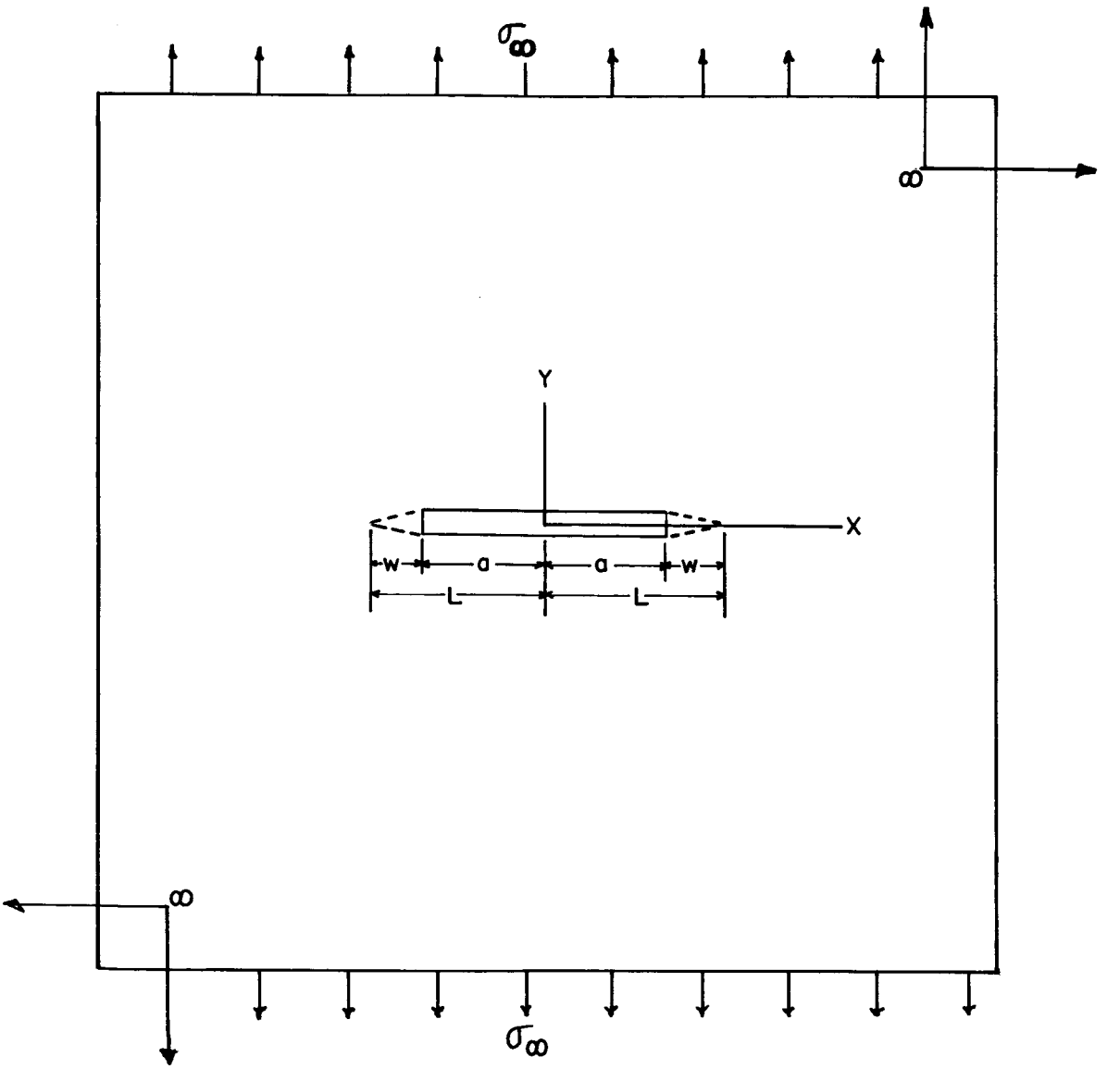

Dugdale's Problem

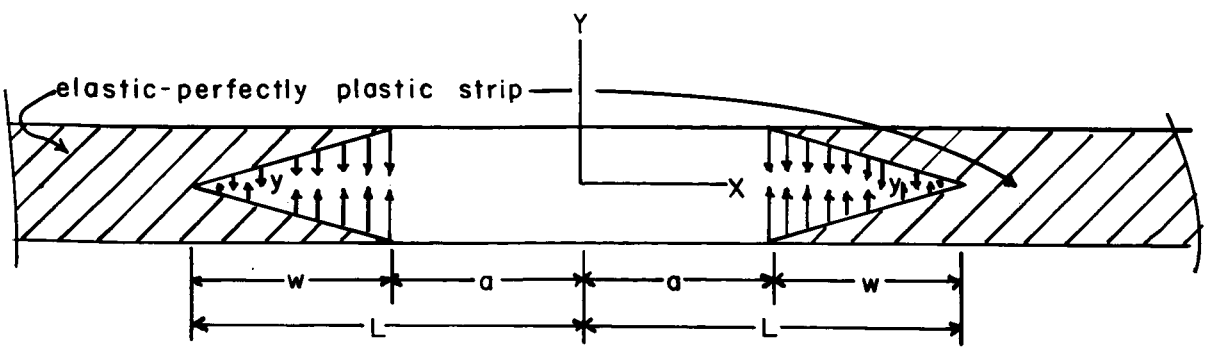

Dugdale's Plastic Enclave Model

FIGURE 4

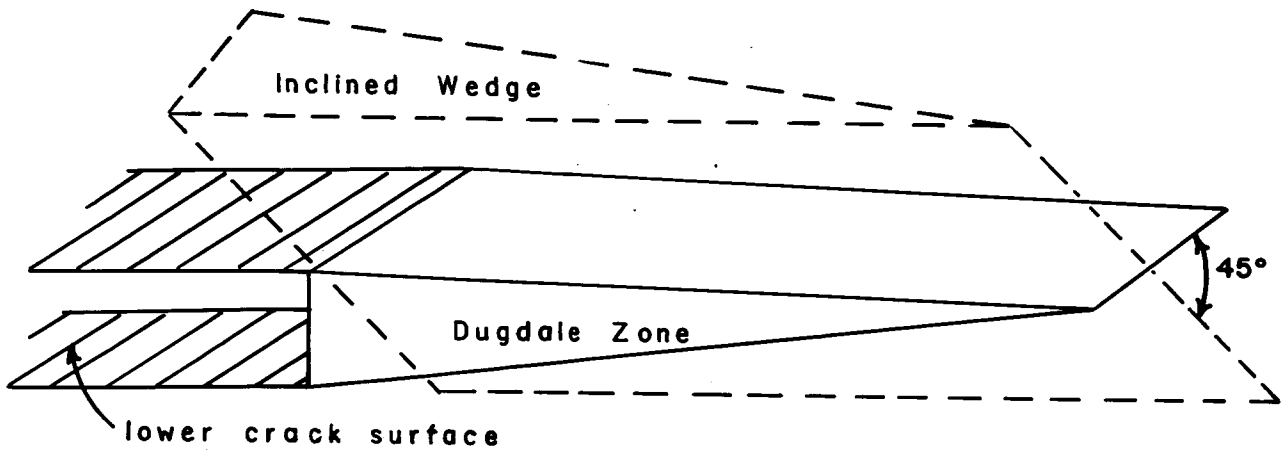

Comparison Between Dugdale Plastic Enclave Model and Experimentally Based 3D Idealized Inclined Wedge Plastic Enclave

FIGURE 5

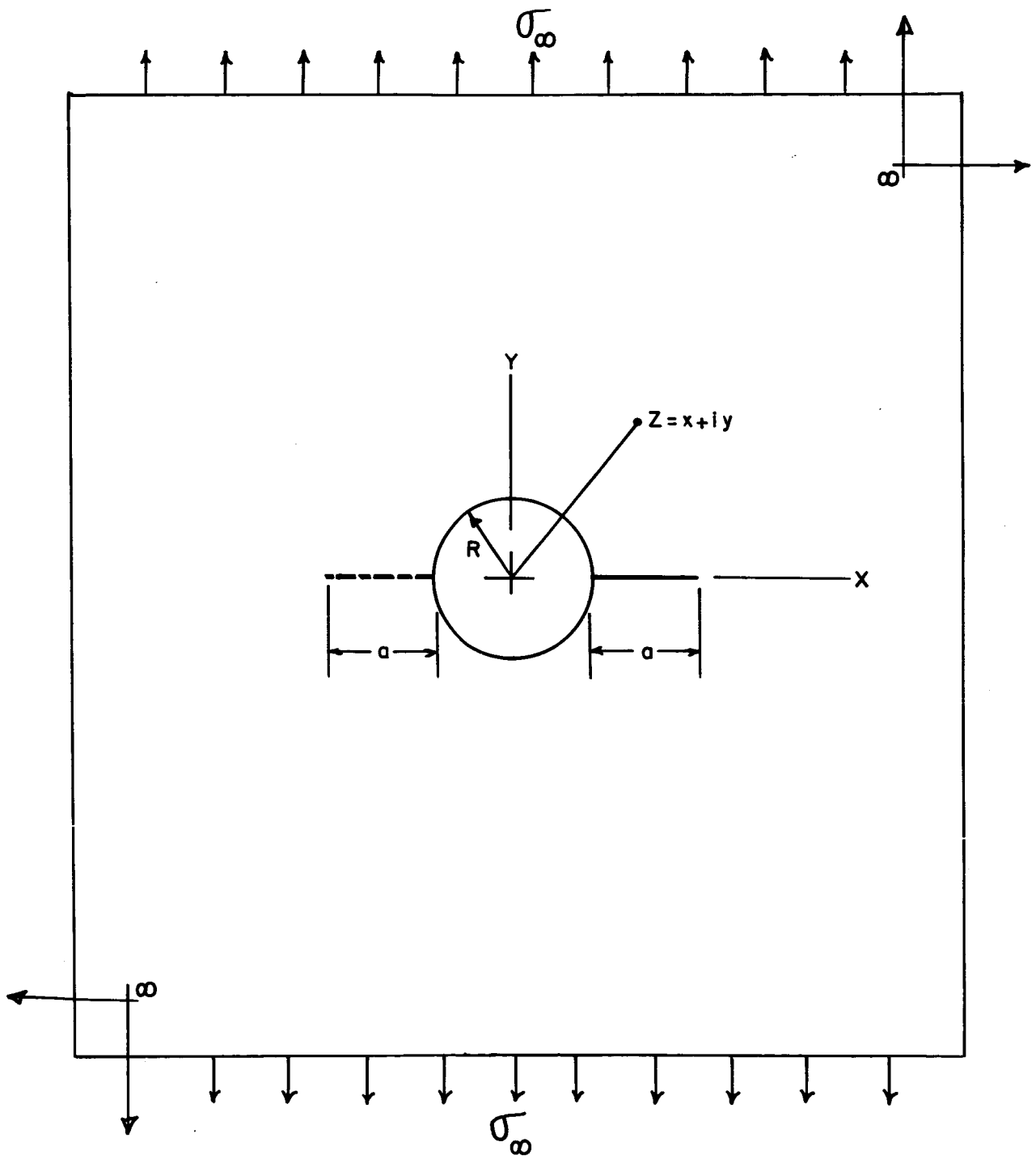

Single and Twin Crack Problems

FIGURE 6

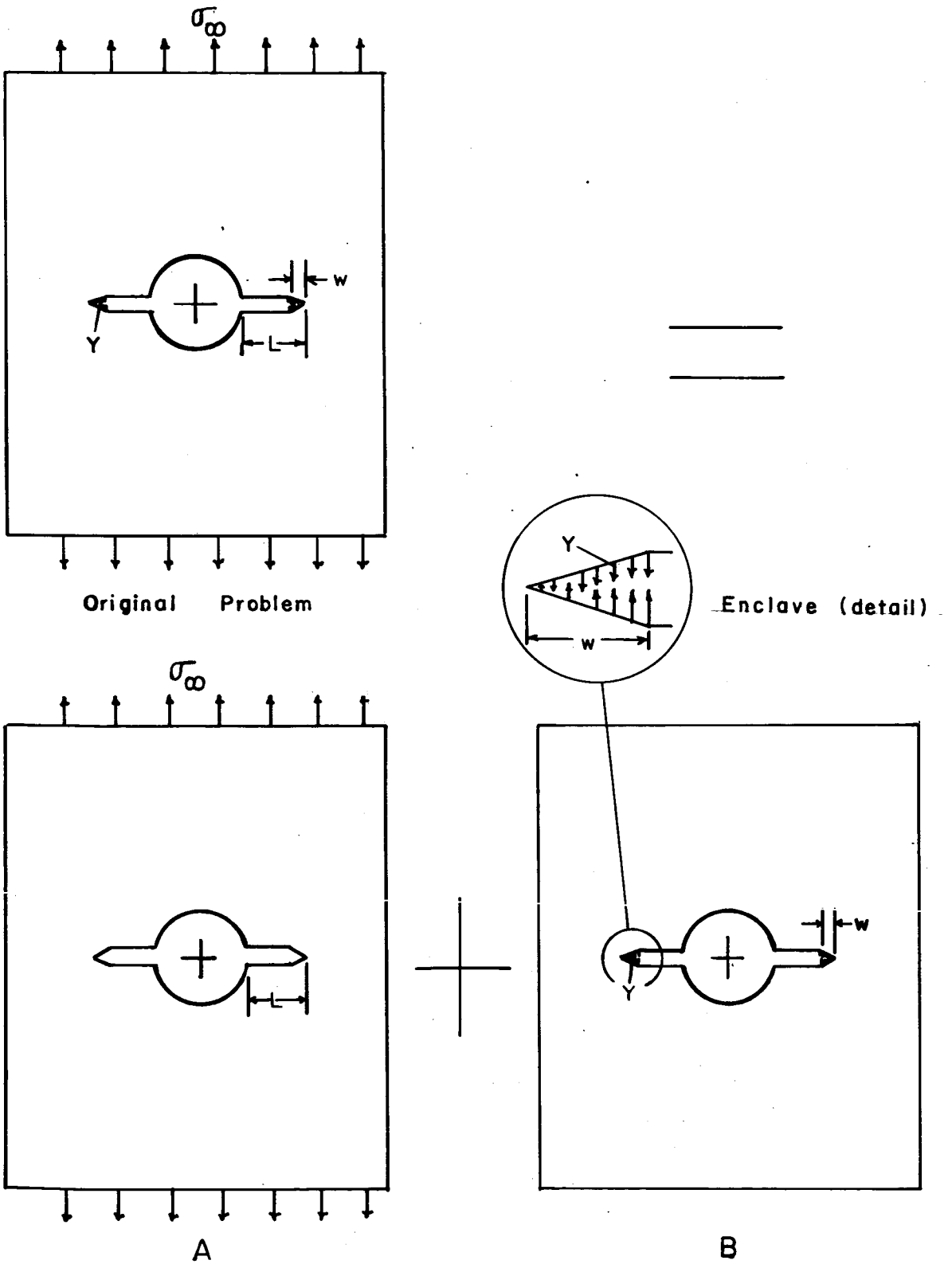

Solution by Linear Superposition

FIGURE 7

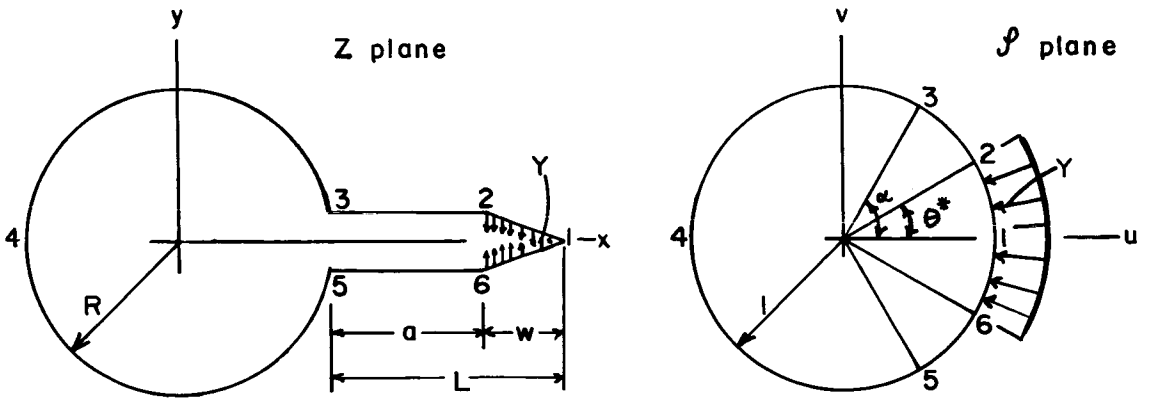

$$Z = \omega_1(\zeta)$$

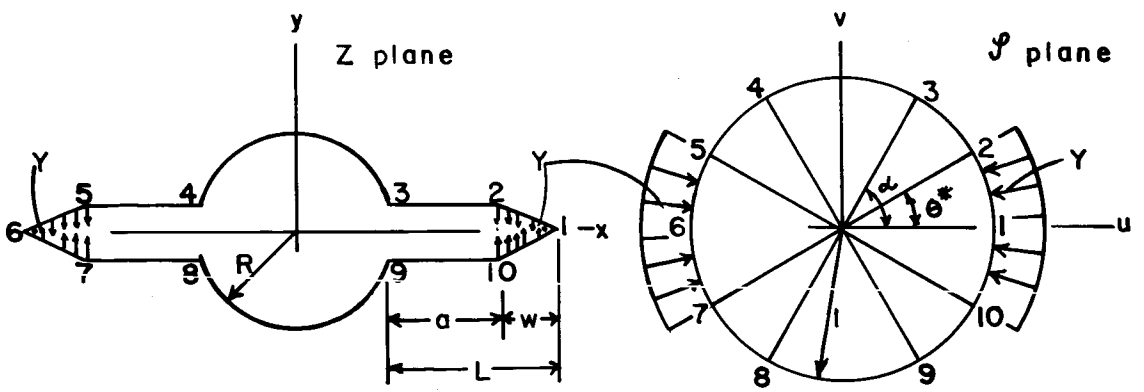

$$Z = \omega_2(\zeta)$$

Mapping Planes for Single and Twin Cracks

FIGURE 8

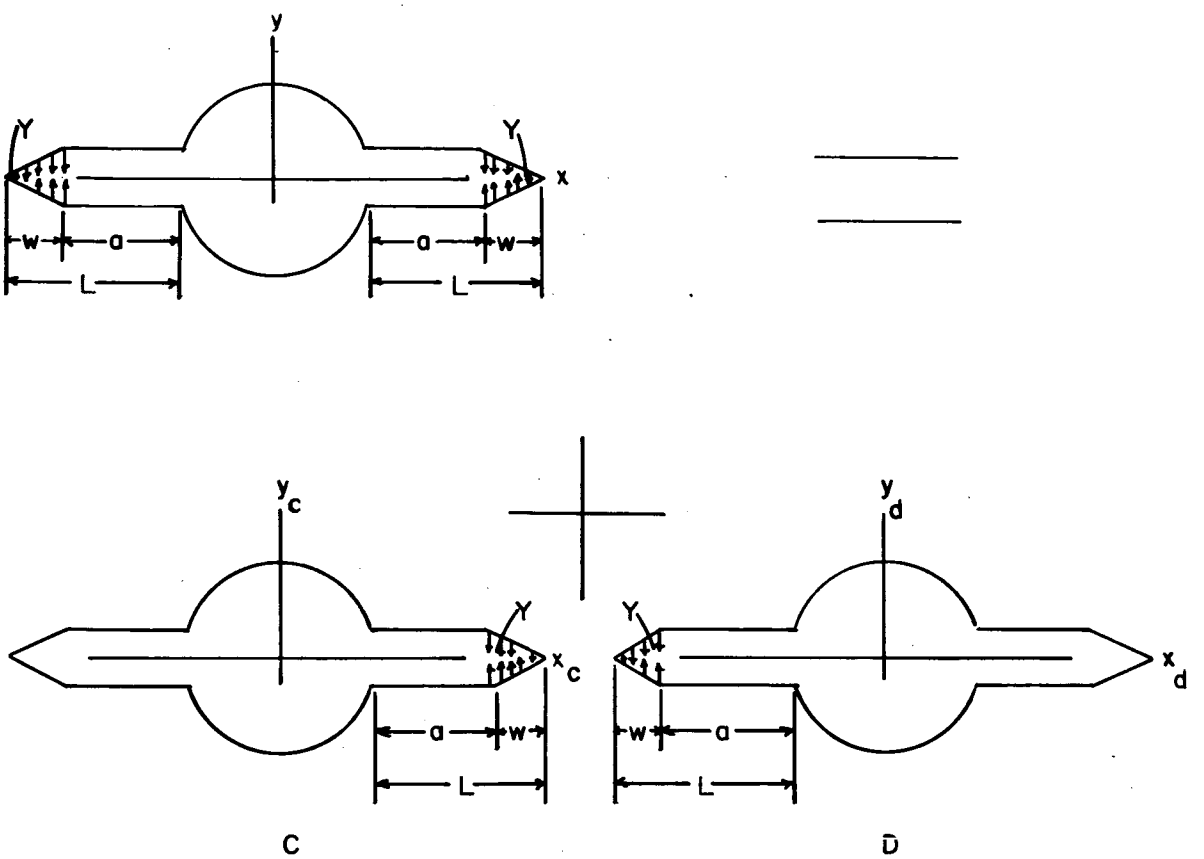

Note - Axes D obtained from axes C by a rotation of π radians.

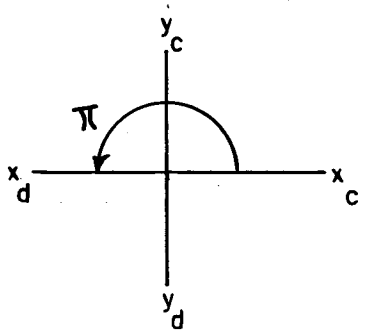

Solution for Twin Problem B by Linear Superposition

FIGURE 9

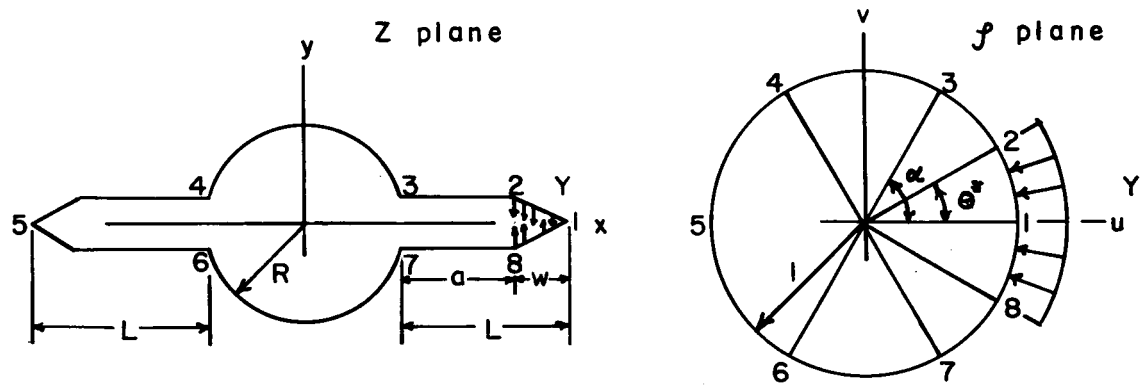

$$Z = \omega_2(\zeta)$$

Mapping Planes for Modified Twin Cracks

FIGURE 10

Plastic Crack Tip Stress Intensity Factors

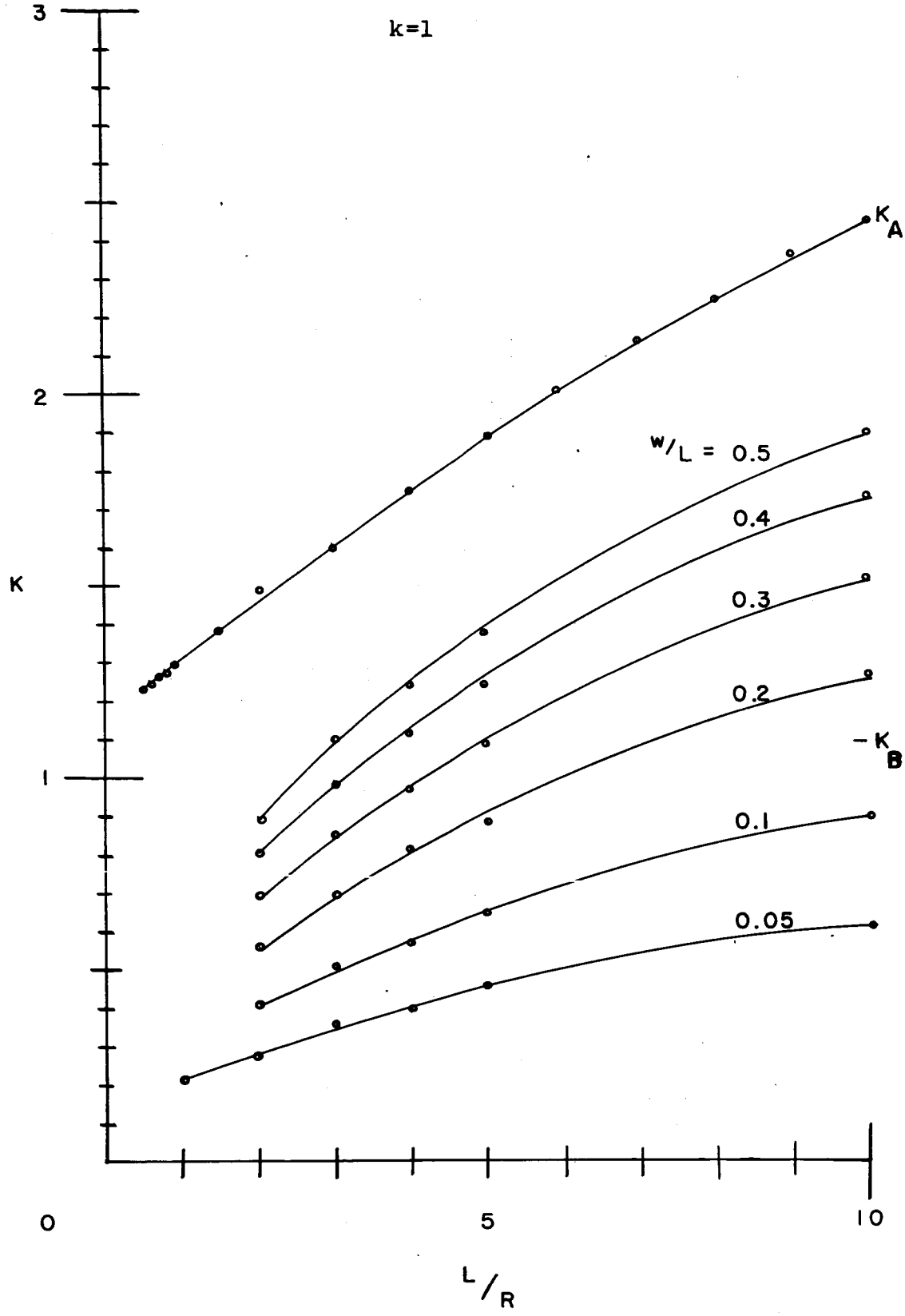

FIGURE 11

Plastic Crack Tip Stress Intensity Factors

k=2

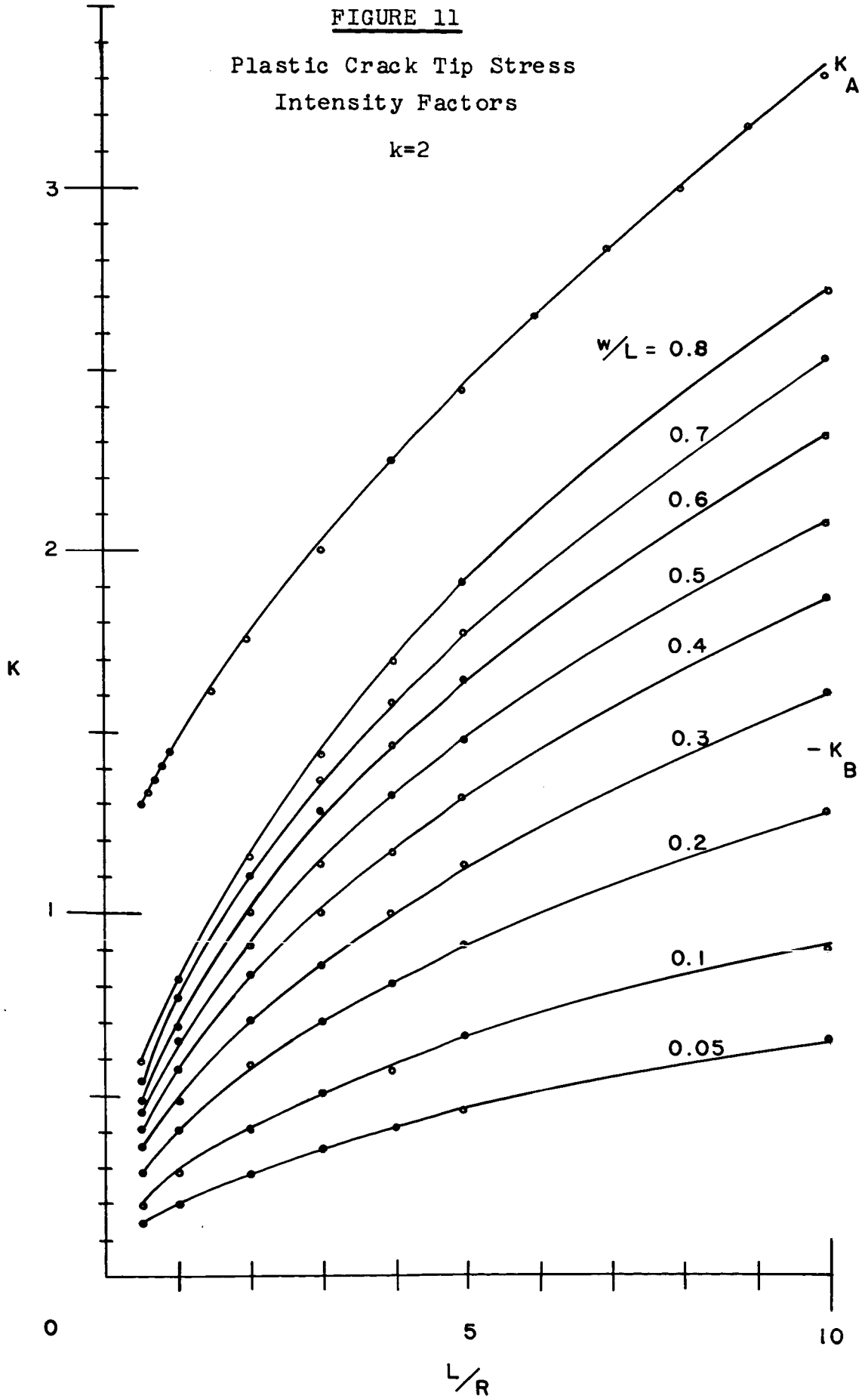

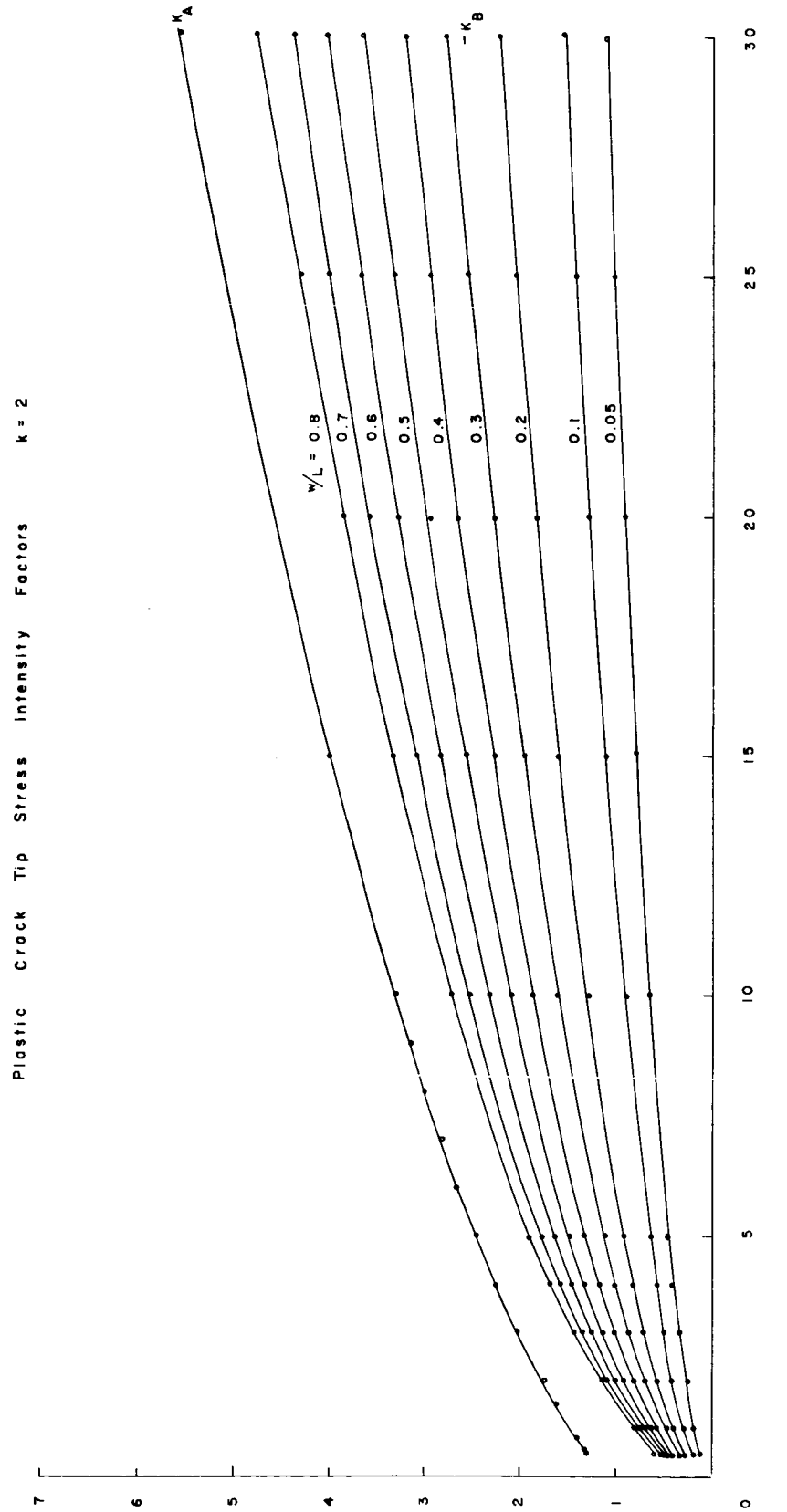
Plastic Crack Tip Stress Intensity Factors k = 2
K_A
$-K_B$
w/L = 0.8
0.7
0.6
0.5
0.4
0.3
0.2
0.1
0.05
L/R
0
5
10
15
20
25
30
1
2
3
4
5
6
7

FIGURE 12

FIGURE 13

Plastic Enclave Sizes

k=1

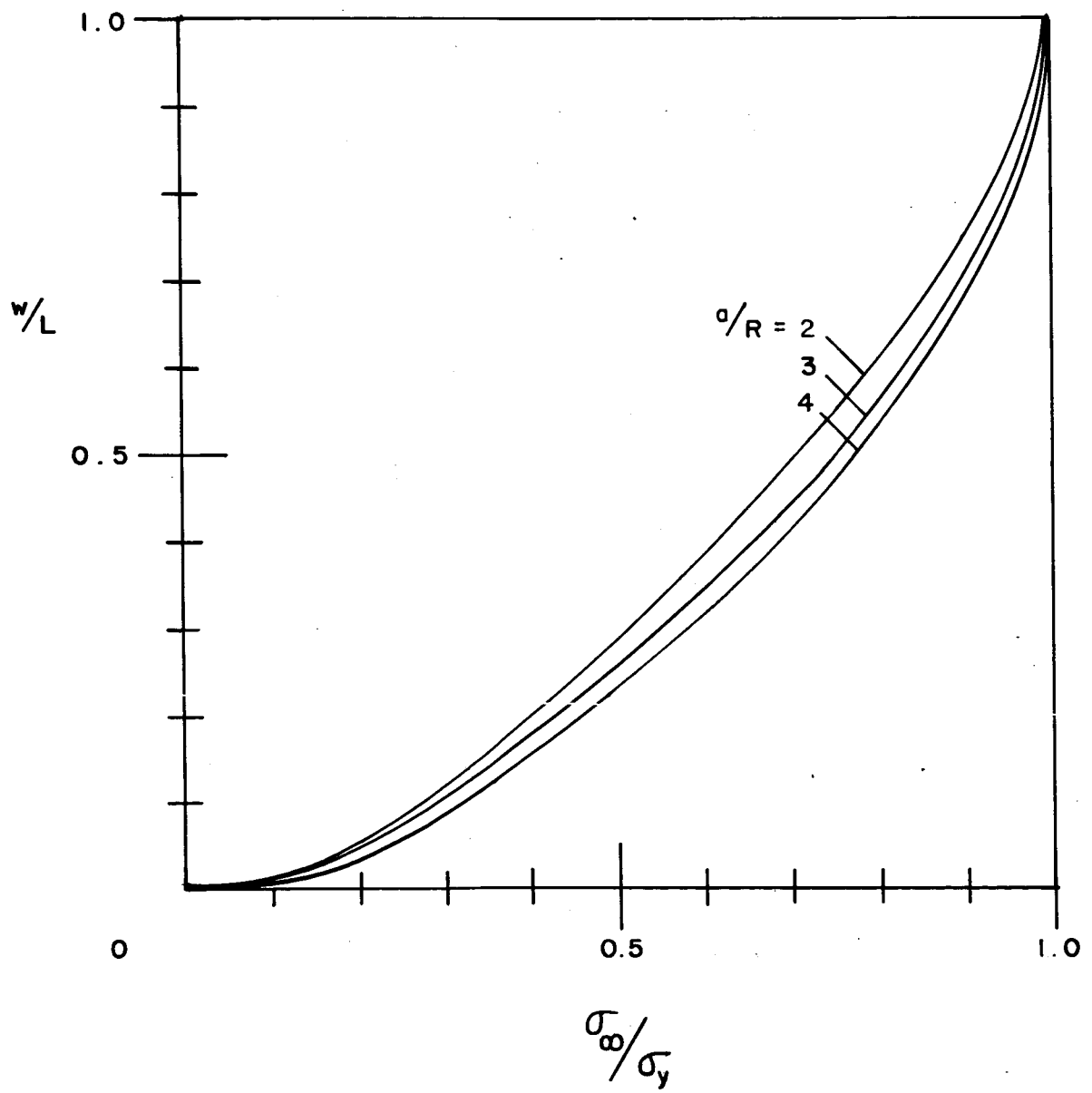

FIGURE 14

Plastic Enclave Sizes

k=2